Journal of Hydrology 620 (2023) 129566

Contents lists available at ScienceDirect

Journal of Hydrology

journal homepage: www.elsevier.com/locate/jhydrol

Research papers

Simulation of the impact of future changes in climate on the hydrology of Bow River headwater basins in the Canadian Rockies

Xing Fang *, John W. Pomeroy

Centre for Hydrology, University of Saskatchewan, 116A-1151 Sidney Street, Canmore, Alberta T1W 3G1, Canada

ARTICLE INFO

This manuscript was handled by Dr marco borga, Editor-in-Chief

Keywords:
Cold regions hydrology
Climate change
Snow
Glacier
Canadian Rockies
Hydrological modelling

ABSTRACT

This study diagnoses the impact of projected changes in climate and glacier cover on the hydrology of several natural flowing Bow River headwater basins in the Canadian Rockies: the Bow River at Lake Louise (~420.7 km^2), the Pipestone River near Lake Louise (~304.2 km^2), the Bow River at Banff (~2192.2 km^2) all of which drain the high elevation, snowy, partially glaciated Central Range, and the Elbow River at Calgary (~1191.9 km^2), which drains the drier Front Ranges and foothills, using models created using the modular, flexible, physically based Cold Regions Hydrological Modelling platform (CRHM). Hydrological models were constructed and parameterised in CRHM from local research results to include relevant streamflow generation processes for Canadian Rockies headwater basins, such as blowing snow, avalanching, snow interception and sublimation, energy budget snow and glacier melt, infiltration to frozen and unfrozen soils, hillslope sub-surface water redistribution, wetlands, lakes, evapotranspiration, groundwater flow, surface runoff and open channel flow. Surface layer outputs from Weather Research and Forecasting (WRF) model simulations for the current climate and for the late 21st century climate under a "business-as-usual" scenario, Representative Concentration Pathway 8.5 (RCP8.5) at 4-km resolution, were used to force model simulations to examine the climate change impact. A projected glacier cover under a "business-as-usual" scenario (RCP8.5) was incorporated to assess the impact of concomitant glacier cover decline. Uncalibrated model simulations for the current climate and glacier coverage showed useful predictions of snow accumulation, snowmelt, and streamflow when compared to surface observations from 2000 to 2015. Under the RCP8.5 climate change scenario, the basins of the Bow River at Banff and Elbow River at Calgary will warm up by 4.7 and 4.5 °C respectively and receive 12% to 15% more precipitation annually, with both basins experiencing a greater proportion of precipitation as rainfall. Peak snow accumulation in Bow River Basin will slightly rise by 3 mm, whilst it will drop by 20 mm in Elbow River Basin, and annual snowmelt volume will increase by 43 mm in Bow River Basin but decrease by 55 mm in Elbow River Basin. Snowcovered periods will decline by 37 and 46 days in Bow and Elbow river basins respectively due to suppressed snow redistribution by wind and gravity and earlier melt. The shorter snowcovered period and warmer, wetter climate will increase evapotranspiration and glacier melt, if the glaciers were held constant, and decrease sublimation, lake levels, soil moisture and groundwater levels. The hydrological responses of the basins will differ despite similar climate changes because of differing biophysical characteristics, climates and hydrological processes generating runoff. Climate change with concomitant glacier decline is predicted to increase the peak discharge and mean annual water yield by 12.23 $m^3 s^{-1}$ (+11%) and 11% in the higher elevation basins of the Bow River but will decrease the mean annual peak discharge by 3.58 $m^3 s^{-1}$ (-9%) and increase the mean annual water yield by 18% in the lower elevation basin of the Elbow River. This shows complex and compensatory hydrological process responses to climate change with the reduced glacier contribution reducing the impact of higher precipitation in high elevation headwaters and drier soil conditions and lower spring snowpacks reducing peak discharges despite increased precipitation during spring runoff in the Front Range and foothills headwaters under a warmer climate.

* Corresponding author.
E-mail address: xing.fang@usask.ca (X. Fang).

https://doi.org/10.1016/j.jhydrol.2023.129566
Received 29 November 2022; Received in revised form 7 March 2023; Accepted 20 April 2023
Available online 25 April 2023

1. Introduction

The Canadian Rockies are a vital source of freshwater to industry, irrigation, and domestic use in the lowland areas and are referred to as the one of the "water towers" of the world (Viviroli et al., 2007). Approximately 70% of annual runoff in major rivers of the Saskatchewan-Nelson River and Peace River systems originates from the Canadian Rockies (Ashmore and Church, 2001), and the high mountain headwaters on the eastern slopes of the Canadian Rockies provide up to 90% of streamflow to downstream users in Canadian Prairie Provinces (Martz et al., 2007). In the eastern slope headwaters of the Canadian Rockies, streamflow is primarily generated from seasonal snowmelt and generally peaks during June (Rood et al., 2008; Whitfield and Pomeroy, 2017), with high flows generated from occasional convective rainfalls and associated rain-on-snow floods (Pomeroy et al., 2016a; Shook, 2016). Glacier meltwater contributes significantly to streamflow during late summer and early fall, and the relative contribution increases upstream towards the Central Ranges, icefields and the Continental Divide (Bash and Marshall, 2014; Comeau et al., 2009; Hopkinson and Young, 1998).

Snowmelt-dominated regions are highly vulnerable to climate change in the 21st century (Adam et al., 2009), and high mountains often respond more rapidly to climate change than do lower altitude regions (Beniston, 2005). Canadian Rockies headwaters have been undergoing warming trends since last century (DeBeer et al., 2016; Valeo et al., 2007). Harder et al. (2015) showed warming of mean temperatures by 2.6 °C and winter minimum temperatures by 3.6 °C at the middle elevations of Marmot Creek, a small Canadian Rockies headwater basin in the Front Ranges, both greater than the regional average warming values for Western Canada reported by Zhang et al. (2000). The fraction of the precipitation as snowfall declines and rainfall ratio increases with the warming air temperatures (Knowles et al., 2006; Shook and Pomeroy, 2012), and this leads to decreases in seasonal snow accumulation (Fang and Pomeroy, 2020; Lapp et al., 2005) and earlier spring snowmelt runoff (Fang and Pomeroy, 2020; Rood et al., 2008) in the Canadian Rockies. Warming climate can cause changes to glacier contributions to streamflow in the southern Canadian Cordillera from glacier retreat (DeBeer et al., 2016; Munro, 2005), resulting in a shift in glacier-fed river flow regimes (Demuth et al., 2008; Marshall et al., 2011). Many headwater rivers draining the Canadian Rockies eastern slopes over the 20th century have shown significant declining trends in annual flow volume (Burn et al., 2004), flood peak and volume (Whitfield and Pomeroy, 2016), and summer flow (Rood et al., 2008). With the predicted climate change in the 21st century (IPCC, 2013) and continuing economic development, irrigation expansion and population growth leading to greater water demand in the downstream regions (Martz et al., 2007), understanding the impacts of projected climate change on the hydrological cycle in the Canadian Rockies is important for managing the water supply from mountain headwaters to downstream regions in the future.

Headwaters draining the Canadian Rockies eastern slopes span a large elevational gradient and contain a range of ecozones including icefield, barren alpine, alpine tundra, subalpine forest, montane forest, rangeland and cultivated prairie. Streamflow generation in these ecozones is usually snowmelt-dominated and is complex and highly variable (Fang and Pomeroy, 2020; Kienzle et al., 2012; Pomeroy et al., 2012; Shea et al., 2021). The large elevational gradient across ecozones influences temperature lapse rates (Wood et al; 2018) and poses orographic effects on precipitation amount and phase (Smith, 2008; Thériault et al., 2015). Complex slope/aspect patterns and high heterogeneity of forest structures in Canadian Rockies are additional factors affecting distribution of wind flow, avalanching, blowing snow, sublimation losses, and irradiance (Conway et al., 2018; MacDonald et al., 2018; Marsh et al., 2012; Musselman and Pomeroy, 2017; Vionnet et al., 2015), and lead to high spatial variability of snow accumulation, snowmelt patterns, evapotranspiration, and runoff generation (DeBeer and Pomeroy, 2017; Ellis et al., 2013; MacDonald et al., 2010; Schirmer and Pomeroy, 2020; Wang et al., 2013; Wayand et al., 2018). Rainfall can be widespread in spring and summer from frontal systems influenced by orography (Pomeroy et al., 2016a) and locally intense where there is convection (Scaff et al., 2021). After rainfall, glacier meltwater is a tertiary streamflow contributor on the eastern slopes and is governed by several factors. The areal distribution of glaciers is highly related to regional temperature and precipitation variabilities (Shea et al., 2004) and is further complicated by local topographic features such as elevation, slope, and aspect (Tennant et al., 2012) and basin-scale processes such as snow redistribution by wind and avalanche (Pradhananga and Pomeroy, 2022a). The interannual variability of glacier mass balance in the headwaters influences streamflow generation and itself is influenced by climate variability and seasonal weather conditions (Demuth et al., 2008).

Several studies have examined the impacts of climate change on snow accumulation, snowmelt, evapotranspiration, glacier mass balance, soil moisture storage, and streamflow in the Canadian Rockies based on simulations of hydrological models driven by future climate scenarios generated by downscaling climate model outputs or perturbing current meteorological conditions (Aubry-Wake and Pomeroy, in review; Fang and Pomeroy, 2020; Farjad et al., 2016; Islam and Gan, 2015; Kienzle et al., 2012; Mahat and Anderson, 2013; Rasouli et al., 2019a, 2022). Hydrological models relying on streamflow calibration by employing the empirical degree-day index approach for simulating snowmelt introduce substantial model uncertainty in predicting future changes due to lack of physically based process representations and possible parameter shifts in future climates or during extreme events such as rain-on-snow (Pomeroy et al., 2013; Walter et al., 2005). Climate models operating at coarse spatial resolution generally have poor precipitation and temperature accuracy in the Canadian Rockies (Rasouli et al., 2019a), and higher resolution atmospheric forcings have been found more suitable for providing more realistic representation of the forcing meteorology for hydrological simulations in the complex mountain terrains (Schirmer and Jamieson, 2015; Vionnet et al., 2015, 2020).

The Cold Regions Hydrological Modelling platform (CRHM; Pomeroy et al., 2007; 2022) consists of a full suite of streamflow generation process representations that are suitable for the cold, snowy climate of the Canadian Rockies, including wind redistribution of snow, snow avalanching, canopy snowfall and rainfall interception, sublimation, drip and unloading from forest canopies, glacier melt, sub-canopy snowmelt, evapotranspiration, infiltration to frozen and unfrozen soils, overland and detention flow, groundwater flow and hillslope subsurface water redistribution. Physically based algorithms in CRHM have been developed from field studies in the region (Aubry-Wake et al., 2022; DeBeer and Pomeroy, 2010; Ellis et al., 2010; Harder and Pomeroy, 2013; MacDonald et al., 2010; Pomeroy et al., 2009; Pradhananga and Pomeroy, 2022a) and have been extensively evaluated in mountain headwater basins (Fang et al., 2013; Fang and Pomeroy, 2016; Pomeroy et al., 2013, 2016b; Pradhananga and Pomeroy, 2022a; Rasouli et al., 2019a). CRHM has also been evaluated in the Earth System Models Snow Model Intercomparison Project and performed relatively well in modelling snowmelt at forest and alpine sites in Canada, France, USA, Japan, Finland and Switzerland (Krinner et al., 2018). A recent application of the Weather Research and Forecasting (WRF) atmospheric model at convection-permitting 4-km resolution provides high resolution forcing meteorology from both the current climate and a future pseudo global warming (PGW) scenario using dynamical downscaling from reanalysis data for large portions of western North America with perturbations from an ensemble of Regional Climate Model (RCM) projections as described by Li et al. (2019). This high-resolution WRF application resolves mountain topography and can capture variations in near-surface meteorology caused by mesoscale orography and convection. CRHM has been driven successfully by these WRF outputs to investigate impacts of climate change on hydrological processes in small

Canadian Rockies and Arctic headwater research basins (Aubry-Wake and Pomeroy, in review.; Fang and Pomeroy, 2020; Krogh and Pomeroy, 2019).

The objectives of this study are to: (1) deploy physically based hydrological models forced with 4-km WRF near-surface meteorology outputs to simulate the cold regions hydrology of several diverse land cover, complex terrain and varied climate Canadian Rockies headwater basins varying between 300 and 2000 km^2; (2) examine and diagnose the future changes in the hydrological processes and response of the region due to the projected climate and glacier changes for these headwater basins. This will provide the most detailed assessment yet of the current hydrology and the expected changes in the headwaters of one of the most water-stressed regions in Canada and the results can be useful for national and provincial park management, climate adaptation policy development, flood mitigation plans and water supply planning and management for large cities and irrigation districts.

2. Methods

2.1. Study area and model domains

The study was conducted in the Bow River at Banff (BRB) and the Elbow River at Calgary (ERC), Alberta, Canada (Fig. 1). Both basins originate in the eastern slopes of the Canadian Rockies and are headwaters of the Bow River that flows eastward and ultimately contributes to the South Saskatchewan River, Saskatchewan River, Lake Winnipeg and the Nelson River flowing to Hudson Bay. Both basins contain a range of alpine rock, alpine tundra, and subalpine forests dominated by conifers; BRB lies entirely in the mountains with approximately 1.7% of the basin area covered by glacier (Bolch et al., 2010), whereas ERC has miniscule glacier coverage but its area consists of 21% grazed grassland and forage cropland (Castilla et al., 2014). Both basins have high surface relief with elevations ranging from 1376 m a.s.l. (above sea level) at the Water Survey of Canada (WSC) streamflow gauge (05BB001) in Banff to just over 3400 m for BRB and from 1075 m at WSC streamflow gauge (05BJ010) in Calgary to just over 3200 m for ERC. The geology in the region is characterized with mainly faulted and folded sedimentary bedrock composed of limestone, sandstone, siltstone, dolostone, and shale (Prior et al., 2013), with surficial soils consisting primarily of highly permeable glaciofluvial and recent alluvial deposits in mountains and foothills and relatively impermeable till and glaciolacustrine deposits in forage cropland region (Bayrock and Reimchen, 1980). The weather for the region is dominated by continental air masses, with long, cold and dry winters and short, warm and sub-humid summers; westerly flow originating from the Pacific Ocean develops warm and dry Chinook (Föhn) conditions that lead to brief periods of air temperature above 0 °C during winter months. Large storms from easterly "upslope" flows can generate deep spring snowpacks or runoff events. Annual precipitation ranges between 800 mm and 1500 mm in higher elevations (Demuth et al., 2008) and is higher in the west, with the observed long-term (1971–2000) mean annual precipitation ranging from 569 mm in Lake Louise at 1524 m, 472 mm in Banff at 1384 m to 412 mm in Calgary International Airport at 1084 m (Environment and Climate Change Canada, 2020). The long-term (1971–2000) mean annual air temperatures are −0.3, 3, and 4.1 °C in Lake Louise, Banff, and Calgary, respectively, with mean monthly air temperatures ranging from −13.8, −9.3, and −8.9 °C in January to 12, 14.6, and 16.2 °C in July for Lake Louise, Banff, and Calgary, respectively (Environment and Climate

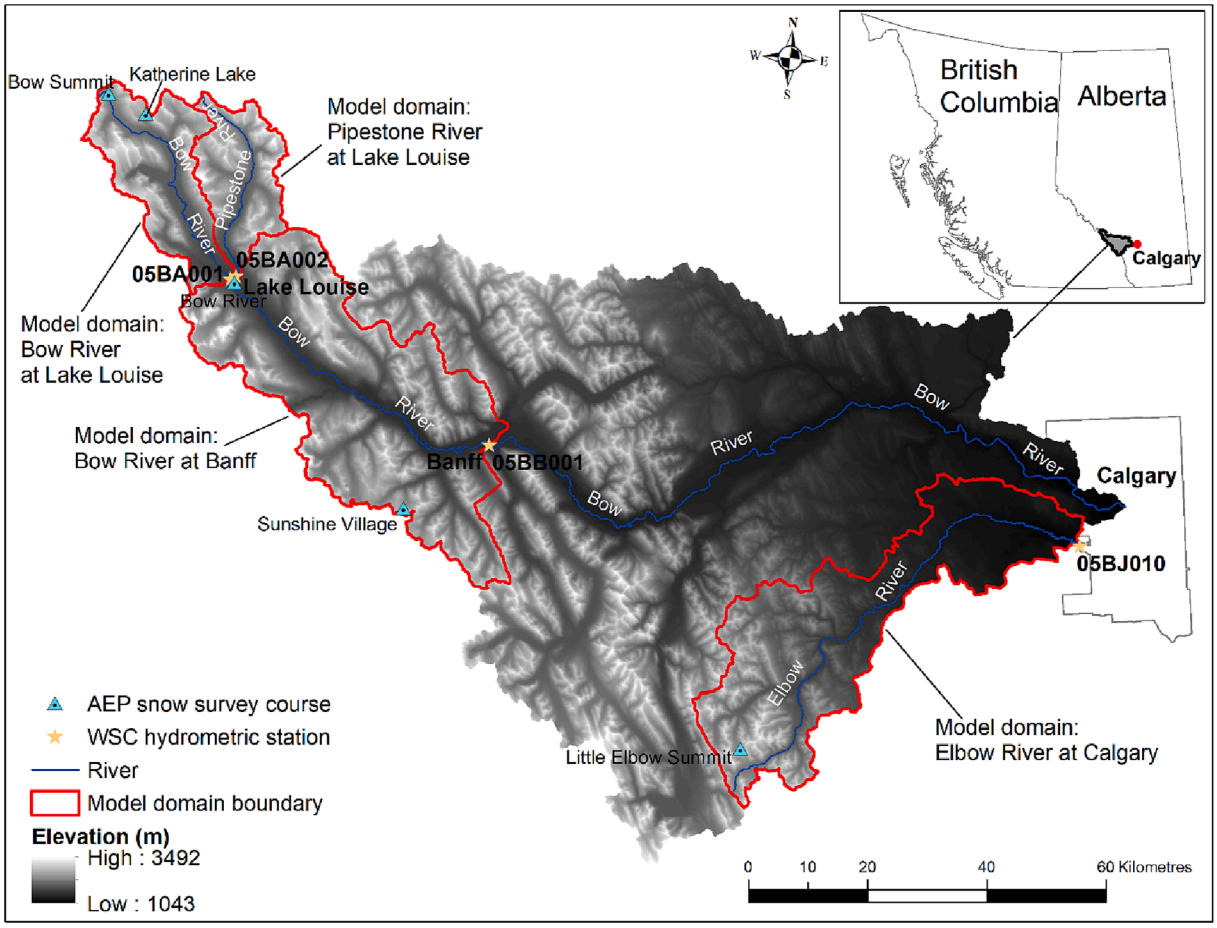

Fig. 1. Location map of Bow River at Banff and Elbow River at Calgary on a 20 m resampled Canadian digital elevation model (cdem), showing Alberta Environment and Parks (AEP) snow survey courses, Water Survey of Canada (WSC) hydrometric stations, and model domains delineated using the cdem.

Change Canada, 2020).

Drainage basins were delineated based on ArcView GIS 3.2 terrain preprocessing (ESRI, 1999) using a resampled 20 m Canadian digital elevation model (cdem) and contain approximately 2192.2 km^2 for BRB above WSC streamflow gauge (05BB001) and 1191.9 km^2 for ERC above WSC streamflow gauge (05BJ010) shown in Fig. 1. In the upper BRB, drainage basins were also delineated for Bow River at Lake Louise (BRLL, ~420.7 km^2) above WSC streamflow gauge (05BA001) and Pipestone River near Lake Louise (PRLL, ~304.2 km^2) above WSC streamflow gauge (05BA002). These delineated drainage basins are the model domains of hydrological model simulations for this study. In addition, 9, 6, 50, and 25 sub-basins were delineated based on the stream segmentation process in GIS terrain preprocessing for the BRLL, PRLL, BRB, and ERC model domains, respectively. Table 1 lists the physiographic information for the model domains, and a sub-basin map for the model domains is provided in the Supplement.

2.2. Hydrological model

2.2.1. CRHM overview

CRHM (Pomeroy et al., 2007; 2022) was used to set up hydrological models for this study. CRHM is an object-oriented, modular and flexible platform for assembling physically based hydrological models. With CRHM, the user constructs a purpose-built model from a selection of possible basin spatial configurations, spatial resolutions and physical process modules of varying degrees of physical complexity. Basin discretization is performed via hydrological response units (HRUs) whose number and nature are selected based on the variability of basin attributes and the level of physical complexity chosen for the model. HRU are landscape units that are assumed to have some common biogeophysical characteristics and hydrological drainage characteristic. The user selects physical complexity in light of hydrological understanding, parameter availability, basin complexity, meteorological data availability, and the objective flux or state to be predicted. Pomeroy et al. (2022) provide a full description of CRHM, and recent updates include Penman-Monteith algorithm in the evaporation module for evapotranspiration from vegetation with seasonal variations in leaf area index and height (Fang and Pomeroy, 2016), a hillslope module for better representation of surface and subsurface runoff including detention flow on hillslopes (Pomeroy et al., 2016b), and a glacier module for simulating glacier melt based on mass and energy balance (Pradhananga and Pomeroy, 2022a).

2.2.2. HRU delineation

Elevation, aspect, slope, and land cover GIS layers were used and intersected in GIS analysis to determine HRUs (Fig. 2). Elevation, aspect, and slope were extracted from the 20 m cdem. Land cover was obtained from the open access Alberta Biodiversity Monitoring Institute (ABMI) Landsat-derived land cover polygon, c. 2000 (Castilla et al., 2014). Glacier cover area was downloaded from the Randolph Glacier Inventory (RGI 3.2) that was mapped using orthorectified Landsat5 Thematic Mapper scenes for years 2004 to 2006 (Bolch et al., 2010), and was used to separate glacier from seasonal snowcover area in the BRB model domain. Pine forest coverage from the Alberta forest species (AVIE) inventory was obtained from Alberta Agriculture and Forestry (2018) and used to separate pine and spruce forest for the ERC model domain. In addition, the water courses in the Alberta drainage network inventory (Alberta Environment and Sustainable Resource Development, 2012) was used to determine river channel valley HRU.

For glacier HRU determinations, seven elevation bands, north-facing, south-facing, and east-facing aspects, and gentle, medium, and steep slope gradients were taken into consideration in order to provide sufficient discretization of snow redistribution, precipitation and temperature gradients, slope-aspect effects on net radiation and slope effects on runoff generation. For rock HRU determinations, upper and lower elevation and north-facing, south-facing, and east-facing aspects were taken into consideration for similar reasons. For alpine tundra, alpine sparse forest, and valley shrubland HRUs, north-facing, south-facing, and east-facing aspects were considered, noting that these landscapes occupy narrow elevation ranges. For all other forest, open water, river valley, developed and exposed HRUs, elevation, aspect, and slope were not used to define HRU areas as slope has little impact on sub-canopy snowmelt (Ellis et al., 2013) and other landscape types occupied valley bottoms. For the ERC model domain, fewer criteria were considered for HRU determination. For glacier, rock, and alpine tundra HRUs, north-facing, south-facing, and east-facing aspects were taken into consideration, but not for the rest of the HRUs. The numbers of delineated HRUs for the model domains are shown in Table 1, and flowcharts of HRU determination and sub-basin HRU information are provided in the Supplement.

2.2.3. Model structure

A set of physically based modules was linked in CRHM to simulate the dominant hydrological processes for the model domains. Fig. 3 shows the schematic setup of these modules, and details of each module are provided in Table 2. For the large model domains in this study, the CRHM model structures were grouped so that a set of physically based modules were assembled with a number of HRUs to represent a sub-basin. The structural grouping was repeated, with same type of sub-basin holding the same module configuration, but differing parameter sets and numbers of HRUs. Muskingum routing was used to route the streamflow output from these sub-basins along the main river channels. Fig. 4 shows the sub-basin group structure for the model domains.

2.2.4. Model parameterization

CRHM parameters values were determined based on field studies in research basins in the Canadian Rockies and similar environments in the boreal forest, subarctic and prairies, by remote sensing or from GIS inventories. For the blowing snow module, fetch length, vegetation height, stalk density, and stalk diameter parameters were determined using methods in previous studies for open prairie environment (Fang et al., 2010) and alpine environments in the Canadian Rockies (Fang et al., 2013; MacDonald et al., 2010). For the canopy module, leaf area index and snow interception capacity parameters were derived from measured values for the similar forest types in the Western Cordillera and boreal forest (Hedstrom and Pomeroy, 1998; Pomeroy et al., 2002, 2012; Schmidt and Gluns, 1991). For the albedo module parameters, albedo of bare ground values were set using measurements from prairie environment (Armstrong, 2011) and boreal forest (Granger and Pomeroy, 1997); the albedo of fresh snow was determined from the observations and recommendations of Male and Gray (1981).

For the glacier module, the glacier HRU area was determined from

Table 1
Area and mean elevation, aspect, and slope as well as basin glacier area and delineated number of sub-basin and HRU for the river basins. Note that the aspect is in degrees clockwise from North.

Model domain	Area (km^2)	Elevation (m a.s.l.)	Aspect (°)	Slope (°)	Basin glacier area (%)	Sub-basin number	HRU number
Bow River at Lake Louise	420.7	2191	152	18	6	9	368
Pipestone at Lake Louise	304.2	2285	171	20	1.7	6	217
Bow River at Banff	2192.2	2138	161	20	1.7	50	1512
Elbow River at Calgary	1191.9	1697	144	13	0.006	25	257

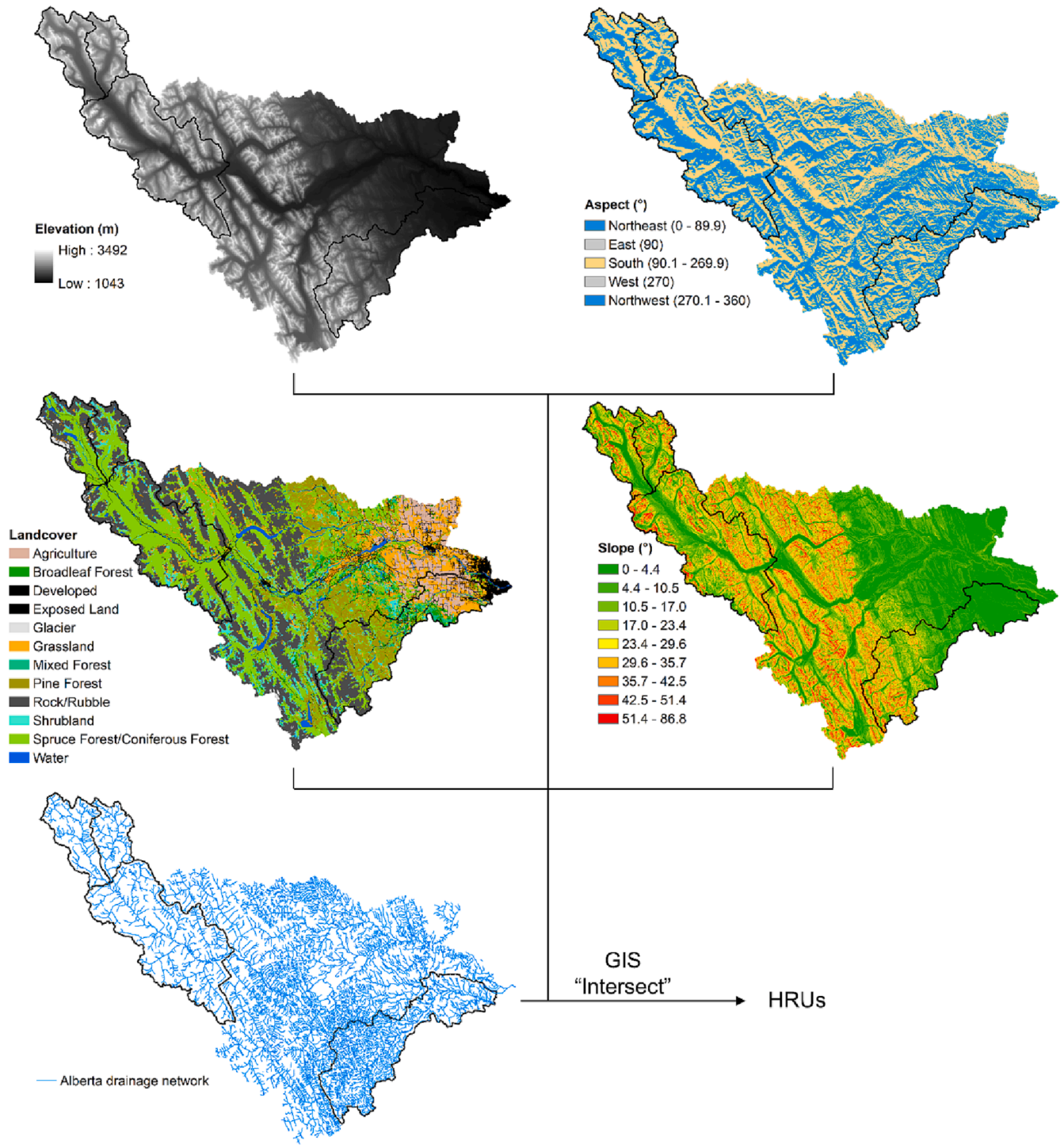

Fig. 2. HRU generation for the model domains from GIS intersect analysis from elevation, aspect, slope, land cover and drainage network GIS layers. Note the solid black line in each layer indicates the model domain boundary shown in Fig. 1.

the RGI 3.2 glacier cover area based on Landsat5 Thematic Mapper scenes for years 2004 to 2006 (Bolch et al., 2010) for the BRB model domain and was derived from the ABMI Landsat-derived ice cover polygon c. 2000 (Castilla et al., 2014) for ERC model domain. The glacier ice thickness parameter was set based on previous studies in the upper Bow River basin (Clarke et al., 2013; Naz et al., 2014). A glacier hydrology model for simulating glacier mass and energy balance in Peyto Glacier (Pradhananga and Pomeroy, 2022a) was instrumental in setting up thickness and density for firn layers, glacier ice density, albedo for firn and ice, and travel time of icemelt, firnmelt and snowmelt through glacier ice, firn and snowpack.

For the soil module, soil depth and porosity parameters were estimated from information on the predominant soil textures in the region (Soil Landscapes of Canada Working Group, 2011). For alpine rock, alpine tundra, and forests HRUs, the water storage capacity in soil and groundwater layers were set based on reported values from long-term studies of Marmot Creek Research Basin (Beke, 1969; Fang et al., 2013). The water storage capacity was set based on values used in the Peyto Glacier hydrology model (Pradhananga and Pomeroy, 2022a) for glacier HRUs and was determined for foothill grassland and cropland

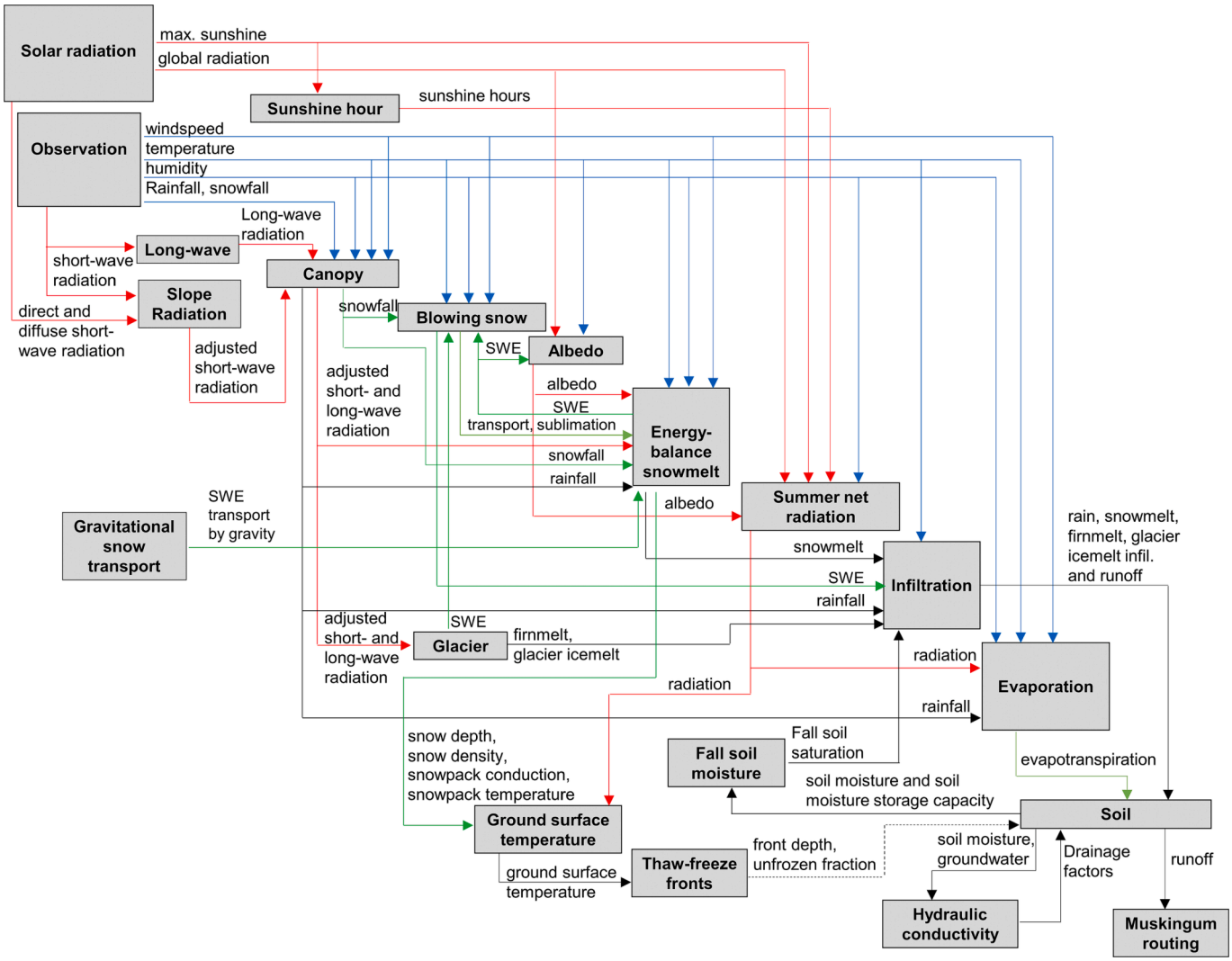

Fig. 3. Module structure of physically based hydrological model showing process and data modules and flow of variables dealing with radiation (red line), meteorology (blue line), evaporation, sublimation and snow (green line) and soil moisture content, ground surface temperature and water (black line). (For interpretation of the references to colour in this figure legend, the reader is referred to the web version of this article.)

HRUs using methods described for prairie environment (Fang et al., 2010).

For the routing module, routing lengths for river channel HRUs were determined from the Alberta drainage network GIS inventory (Alberta Environment and Sustainable Resource Development, 2012) and for non-river channel HRUs from the modified Hack's law for length-area relationship reported by Fang et al. (2010). Manning's equation was used to calculate the average streamflow velocities based on longitudinal channel slope, Manning's roughness coefficient, and the channel hydraulic radius as parameters. The longitudinal channel slope of a HRU or a sub-basin was estimated from the average slope of the HRU or sub-basin. Manning's roughness coefficient was approximated based on surface cover and channel conditions using values reported by Chow (1959). The hydraulic radius was determined from Chow's lookup table using channel shape and channel depth as criteria. The routing sequence within a sub-basin was set using a routing distribution parameter to represent the typical flow sequence amongst HRUs (Fang et al., 2010; Fang et al., 2013), while the routing sequence amongst sub-basins followed the channel flow order downstream through the basin. Both routing sequences are provided in the Supplement. Values for the key parameters are listed in the Supplement tables.

2.3. WRF model

The WRF model Version 3.6.1 (Li et al., 2019) was used to develop the forcing meteorological fields used to drive the CRHM hydrological models. This version of WRF simulates weather systems at convection-permitting 4-km resolution and can capture variations in near surface meteorology caused by mesoscale orography. Model outputs from two 15-year periods of WRF experiments were available, consisting of a control (CTL) simulation and a PGW simulation. The CTL simulation was forced with boundary condition from a 6-hour ERA-Interim reanalysis data (Dee et al., 2011) and corresponds to a retrospective period of 2000–2015. The PGW simulation was forced with the 6-hour ERA-Interim reanalysis data plus a climate perturbation; the climate perturbation was based on 19-model ensemble mean change from the fifth phase of the Coupled Model Intercomparison Project (CMIP5; Taylor et al., 2012) under a "business-as-usual" forcing scenario: Representative Concentration Pathway 8.5 (RCP8.5; van Vuuren et al., 2011). The PGW is equivalent to a future period of 2084–2099. More details of WRF model are provided by Li et al. (2019). There are 49 and 25 grids respectively of the 4-km WRF model outputs used to force the hydrological model simulations for BRB and ERC model domains; out of the 49 grids in BRB model domain, 9 and 6 WRF grids respectively are for BRLL and PRLL model domains. Information on these WRF grids is provided in

Table 2
Description of modules used for simulating hydrological processes in CRHM.

Module	Description
1. Observation	Reads the input meteorological data (temperature, wind speed, relative humidity, precipitation, and radiation), adjusts temperature with environmental lapse rate and precipitation with elevation, and provides these inputs to other modules
2. Solar radiation	Calculates the theoretical global radiation, direct and diffuse solar radiation, as well as maximum sunshine hours based on latitude, elevation, ground slope, and azimuth (Garnier and Ohmura, 1970); provides radiation inputs to the sunshine hour module and the summer net radiation module
3. Sunshine hour	Estimates sunshine hours from shortwave irradiance to a level surface and maximum sunshine hours; generates inputs to the summer net radiation module
4. Slope radiation	Estimates shortwave irradiance to a slope using measurement of shortwave irradiance on a level surface. The measured shortwave irradiance from the observation module and the calculated direct and diffuse shortwave irradiance from the radiation module are used to calculate the ratio for adjusting the shortwave irradiance on the slope
5. Longwave	Estimates longwave irradiance using measured or estimated shortwave irradiance (Sicart et al., 2006); provides input to the canopy module
6. Canopy	Estimates the snowfall and rainfall intercepted by the forest canopy, updates the sub-canopy snowfall and rainfall, and calculates shortwave and longwave sub-canopy irradiance (Ellis et al., 2010). This module has options for an open environment with no canopy effects, a small forest clearing gap, or a full forest canopy
7. Blowing snow	Simulates the inter-HRU wind redistribution of snow transport based on surface aerodynamic roughness and blowing snow sublimation losses throughout the winter period (Pomeroy and Li, 2000)
8. Albedo	Estimates snow albedo throughout the winter and into the melt period and also indicates the beginning of melt for the energy-balance snowmelt module (Verseghy, 2012)
9. Gravitational snow transport	Simulates the inter-HRU snow transport by gravity along steep slope and topographic driven distribution of snow (Bernhardt and Schulz, 2010)
10. Energy-balance snowmelt	Simulates the mass and energy balance of snowpack based on a version of the SNOBAL model (Marks et al., 1998) and estimates snowmelt and flow through snow using the energy balance of radiation, sensible heat, latent heat, ground heat, advection from rainfall, and the change in internal energy for snowpack layers consisting of a top active layer and layer underneath it
11. Glacier	Estimates icemelt from glacier ice and firnmelt from firn layers based on energy-balance model and handles the movements of icemelt, firnmelt and snowmelt through glacier ice, firn and snowpack using a simple lag and route method (Pradhananga and Pomeroy, 2022a)
12. Summer net radiation	Calculates the snow-free net all-wave radiation from the estimated shortwave radiation and the estimated longwave radiation using air temperature, vapour pressure, and actual sunshine hours (Granger and Gray, 1990) and provides input to the evaporation and ground surface temperature modules
13. Infiltration	Estimates snowmelt infiltration into frozen soils using Gray's parametric snowmelt infiltration algorithm (Zhao and Gray, 1999) and rainfall infiltration into unfrozen soils based on soil texture and ground cover (Ayers, 1959); links moisture content to the soil column in the soil module
14. Fall soil moisture	Estimates fall soil moisture status based on the amount of soil moisture and the maximum soil moisture storage in the soil column and provides the initial fall soil saturation for the infiltration module
15. Evaporation	Estimates actual evapotranspiration from unsaturated surfaces using Penman-Monteith evapotranspiration algorithm (Monteith, 1965) with a Jarvis-style resistance formulation (Verseghy, 1991) and evaporation from saturated surfaces using Priestley and Taylor evaporation expression (Priestley and Taylor, 1972); modifies
16. Soil	Estimates soil moisture balance, groundwater storage, surface depressional and near-surface detention storages; calculates surface runoff and runoff for two soil layers, a groundwater layer, surface depressions, and a near-surface detention layer (Fang et al., 2010; Pomeroy et al., 2016b), linking to thaw-freeze fronts to account for permafrost
17. Hydraulic conductivity	Estimates drainage factors based on Darcy's law for unsaturated hydraulic conductivity using Brooks and Corey relationship (Fang et al., 2013) and provides the drainage factors used in soil module.
18. Thaw-freeze fronts	Simulates the freezing and thawing fronts in seasonal frost or permafrost soil based on a modified Stefan's heat flow equation for user specified number of soil layers (Xie and Gough, 2013; Krogh et al., 2017); provides status of thawing and freezing fronts for soil module
19. Ground surface temperature	Calculates the ground surface temperature using air temperature and thermal conductivity and energy of snowpack during snowcover period based on conduction approach (Luce and Tarboton, 2010) and using air temperature and net radiation for snow-free period based on radiative-conductive-convective approach (Williams et al., 2015); provides ground surface temperature input for thaw-freeze fronts module
20. Muskingum routing	Routes runoff between HRUs and to the sub-basins outlet using Muskingum method (Chow, 1964), allowing one HRU to route runoff to one or multiple HRUs (Fang et al., 2010); routes subsurface and groundwater flows using Clark's lag and route algorithm (Clark, 1945)

the Supplement.

2.4. Hydrological simulations

Hydrological model simulations were driven by the WRF outputs of near-surface meteorological variables: including air temperature, vapour pressure, wind speed, shortwave irradiance, and precipitation, where the air temperature and vapour pressure were used to estimate relative humidity required by CRHM. Three types of simulations were conducted:

Reference simulation: use the WRF CTL outputs for the 15-water year (WY) simulation in the current period (i.e. 1 October 2000 to 30 September 2015) with the current glacier coverage from the RGI 3.2 Inventory (Bolch et al., 2010).

Climate scenario simulation: use the WRF PGW outputs for the 15-WY simulation in the future period (i.e. 1 October 2084 to 30 September 2099) with glacier ice volume reduced by 99% from the reference simulation, a value guided by the RCP8.5 glacier projection in the southern Canadian Rockies at the end of the 21st century and a glacier dynamics model (Clarke et al., 2015). The RCP8.5 climate and deglaciation projections are considered a high emission climate change scenario and were used to examine the hydrological impact of the worst-case scenario.

Glacier falsification simulations: Falsification 1 uses the WRF CTL outputs for the 15-WY simulation in the current period with the glacier ice volume reduced by 99% from the reference simulation; Falsification 2 uses the WRF PGW outputs for the 15-WY simulation in the future period with the current glacier coverage.

Snow accumulation and streamflow from the reference simulation were evaluated against observed snow accumulation from Alberta Environment and Parks (AEP) snow survey courses and streamflow from Environment and Climate Change Canada's Water Survey of Canada (WSC) hydrometric stations. Statistical indexes used to evaluate model simulations were the Nash–Sutcliffe efficiency (NSE) (Nash and Sutcliffe, 1970), RMSD, normalised RMSD (NRMSD), and model bias (MB)

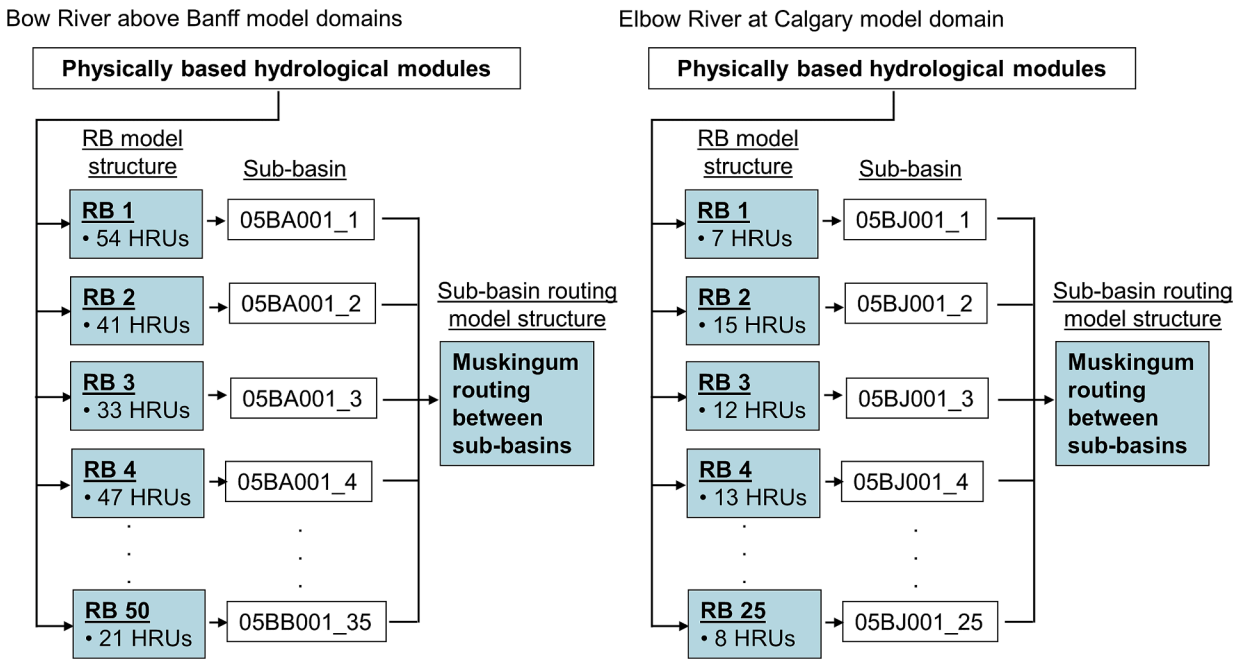

Fig. 4. Sub-basin group structure for the model domains. Sub-basins are simulated by the model structure "representative basin" (RB) group, and the model structure, Muskingum Routing, connects all RBs. Note not all sub-basins in the river basins are shown due to their large number, and information for all sub-basins is provided in the Supplement.

calculated as per Fang et al. (2013).

2.5. Hydrological index calculations

Several indices characterising the hydrological regime were examined, including the rainfall ratio (RR), snow hydrology ratio (SHR), snow damming ratio (SDR), and runoff coefficient (RC). RR is the cumulative rainfall divided by cumulative precipitation over a water year (WY) starting from 1 October to 30 September of the following year, with RR greater than 0.5 indicating a rainfall-dominated precipitation regime and RR less than 0.5 indicating a snowfall-dominated precipitation regime. SHR is the cumulative snowmelt volume divided by cumulative precipitation over a WY, with the higher SHR indicating greater influence of snow hydrology on runoff. SDR is adapted from López-Moreno et al. (2020) to characterise the snowpack storage capacity that effectively "dams" precipitation, compared to rainfall-runoff, during cold months, and is estimated by the maximal difference between the cumulative fractions of precipitation and runoff for a WY starting from 1 October and ending 30 September of the following year, with a higher SDR indicating that the seasonal snowpack acts to a greater degree as a natural water reservoir over the winter until snowmelt occurs. RC is the cumulative streamflow volume divided by cumulative precipitation over a WY and normally varies between 1 and 0, with the higher RC reflecting better capability of basin to convert precipitation volume to streamflow volume.

3. Results

3.1. Model evaluations

CRHM simulations of the snow accumulation (SWE) using the reference simulation were compared to the monthly SWE measurements from the following AEP snow courses: Bow Summit (2031 m a.s.l.), Katherine Lake (2380 m a.s.l.), Bow River Lake Louise (1580 m a.s.l.), Sunshine Village (2230 m a.s.l.), and Little Elbow Summit (2120 m a.s.l.) (Fig. 5). Simulated SWE from the HRUs corresponding to the location and land cover of these snow courses include the conifer forest (2120 m a.s.l.) and valley shrubland (2000 m a.s.l.) HRUs from sub-basin 2 in BRB (Fig. 5a), the lower rock (2211 m a.s.l.) HRU from sub-basin 4 in BRB (Fig. 5b), the river valley (1553 m a.s.l.) HRU from sub-basin 9 in BRB (Fig. 5c), the alpine tundra (2322 m a.s.l.) HRU from sub-basin 43 in BRB (Fig. 5d), and the regenerated forest (2149 m a.s.l.) HRU from sub-basin 3 in ERC (Fig. 5e). The model generally reproduced snow accumulation and ablation patterns that were comparable to the measured SWE, with the noticeable overestimation of SWE in most simulation years (i.e. 2001, 2003–2009, 2015) compared to SWE measurements at the Little Elbow Summit snow course (Fig. 5e) and underestimation of SWE in some simulation years (i.e. 2006, 2008, 2012) compared to Sunshine Village snow course-measured SWE (Fig. 5d). For the 15-WY period (2000–2015), model simulations reasonably predicted SWE when compared to snow courses in BRB, with MB ranging from −0.07 at Sunshine Village to 0.25 at Katherine Lake, RMSD ranging from 52 mm at Bow River Lake Louise to 132 mm at Katherine Lake, and NRMSD varying from 0.21 at Sunshine Village to 0.32 at both Katherine Lake and Bow River Lake Louise (Fig. 5). Simulations differed to a much greater degree from observations at the Little Elbow Summit snow course in ERC, with MB of 0.51, RMSD of 175 mm, and NRMSD of 0.72. The high MB value suggesting 51% overestimation compared to the observed SWE have resulted from errors in the WRF forcing data and modelling of blowing snow redistribution into the regenerated forest HRU that did not occur in nature.

Model evaluation was also conducted using the CRHM-simulated streamflow from the reference simulation and the outlet streamflow discharge measured at WSC gauges: Bow River at Banff (BRB), Pipestone River at Lake Louise (PRLL), Bow River at Lake Louise (BRLL), and Elbow River at Calgary (ERC) for 15 water years (2000–2015) (Fig. 6). These gauges have no water management upstream and are suitable for a natural flow simulation such as used here. They also represent high elevation, steep, partly glaciated and lake dominated environments (BRLL), high elevation, steep environments (PRLL), nested within the mixed alpine, subalpine, montane, valley bottom and high elevation environments with lakes and a small glacier coverage of the BRB, and contrasting montane forest and alpine front ranges and foothills environments of the ERC. The model reasonably simulated the daily

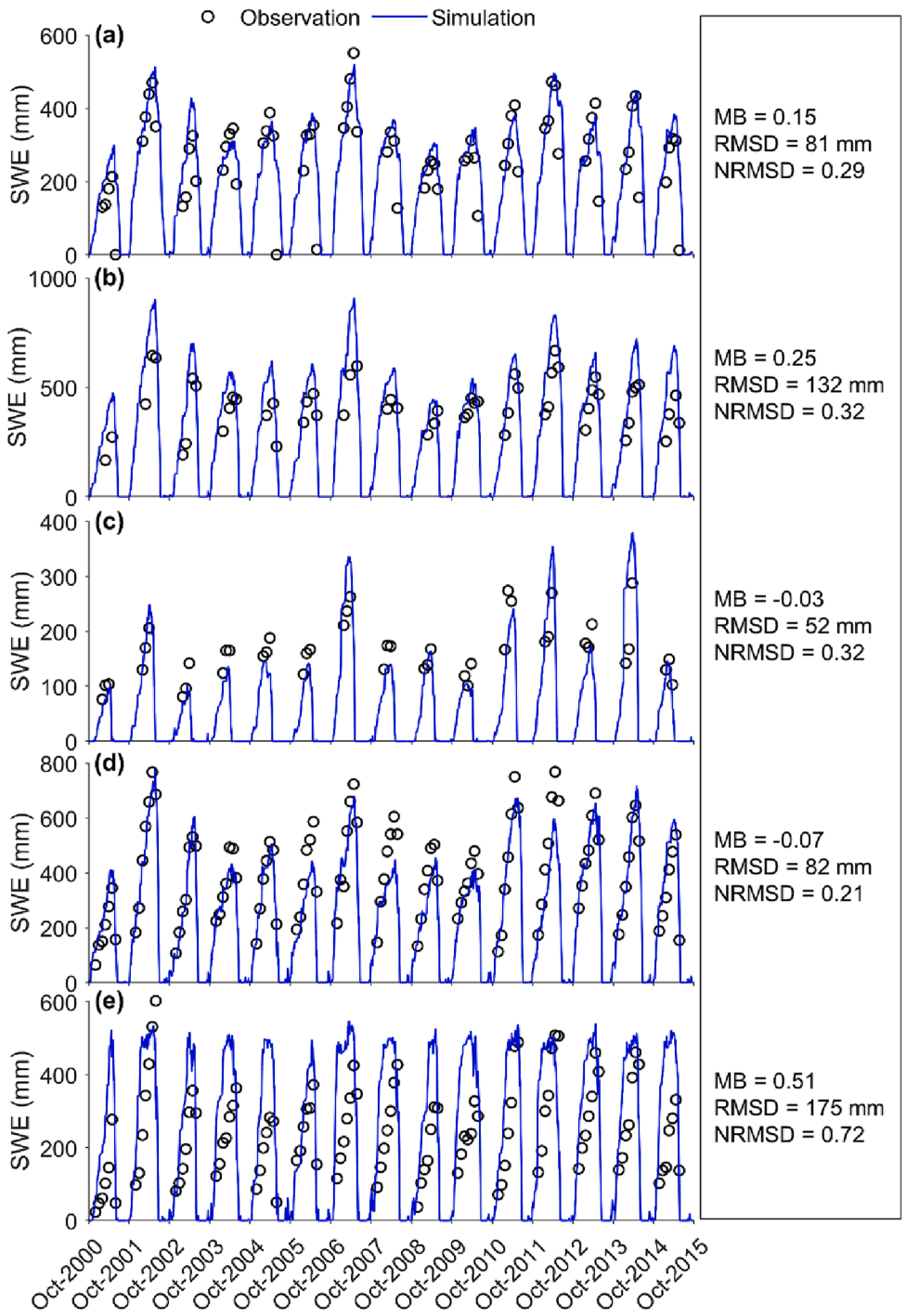

Fig. 5. Comparison of the measured and simulated snow accumulation (SWE) for 2000–2015 at sites in the Bow River and Elbow River basins. (a) Bow Summit, (b) Katherine Lake, (c) Bow River Lake Louise, (d) Sunshine Village, and (e) Little Elbow Summit.

streamflow at the BRB, and the 15-WY NSE, MB, RMSD, and NRMSD were 0.75, −0.13, 20.7 $m^3 s^{-1}$, and 0.57, respectively (Fig. 6c). For the two sub-basins in upper BRB, the model achieved better streamflow simulation for PRLL, with values of 0.70, −0.02, 4.3 $m^3 s^{-1}$, 0.73 for NSE, MB, RMSD, and NRMSD, respectively (Fig. 6b); whilst the 15-WY NSE, MB, RMSD, and NRMSD for BRLL were poorer at 0.38, −0.25, 8.9 $m^3 s^{-1}$, and 0.52, respectively (Fig. 6a). For the ERC, the simulation could capture daily streamflow for most years but missed peak flows in two flood years (i.e. 2005 and 2013) and two high flow years (i.e. 2008 and 2011), and so the 15-WY NSE, MB, RMSD, and NRMSD were 0.38, −0.20, 15.3 $m^3 s^{-1}$, and 1.32, respectively (Fig. 6d). This suggests errors in precipitation forcing from WRF over this basin. Comparison of the 15-WY mean daily streamflow for the BRLL shows that the model underestimated flow from middle May to early September and overestimated flow in October (Fig. 6e), which possibly resulted from underestimation of precipitation in WRF and model's delay in routing flow from glacier melt water, leading to poor NSE and MB values. Comparison with the 15-WY mean daily observed streamflow for the ERC reveals that the model underestimated flow from late May to early July and displayed a flashier hydrograph from early August to middle September (Fig. 6h). This may be attributed to underestimation of precipitation in WRF and/or errors in the model's simulation of rainfall generated streamflow. The

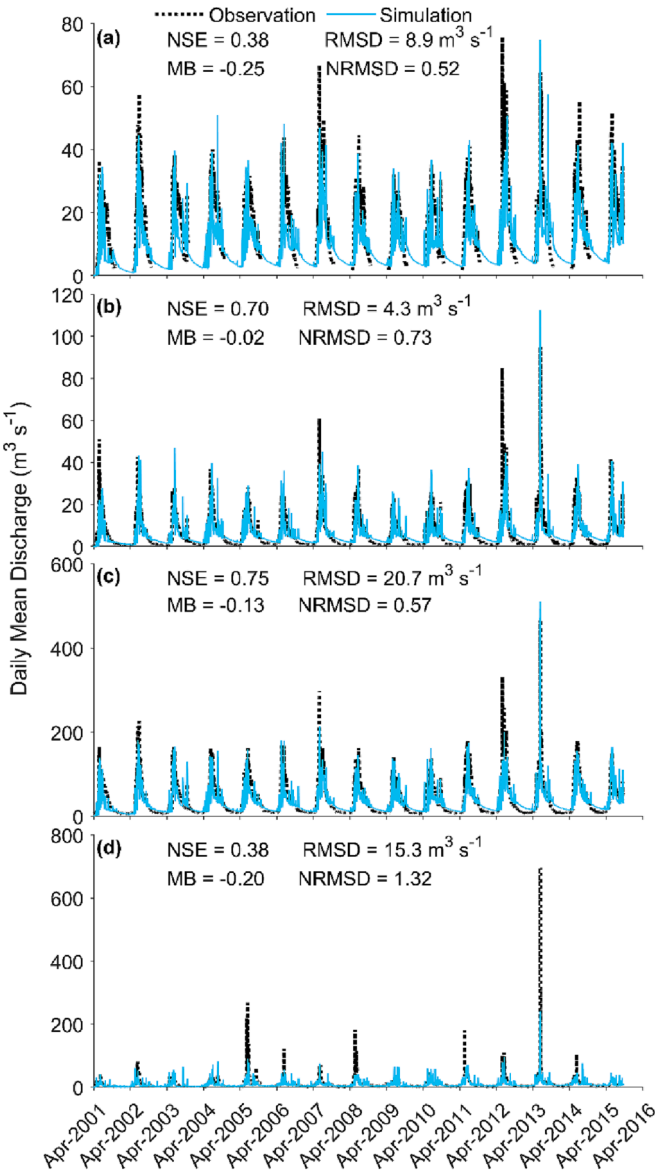

Fig. 6. Comparison of the observed and simulated daily streamflow over 15 water years (i.e. 2000–2015) for (a) Bow River at Lake Louise (05BA001), (b) Pipestone River at Lake Louise (05BA002), (c) Bow River at Banff (05BB001), and (d) Elbow River at Calgary (05BJ010); comparison of the observed and simulated 15-water year mean daily streamflow for (e) Bow River at Lake Louise, (f) Pipestone River at Lake Louise, (g) Bow River at Banff 001), and (h) Elbow River at Calgary. The line in (e-h) represents the mean and the shadow represents the standard deviation of the 15-water year streamflow.

Elbow River Basin is composed of steep, narrow mountain valleys that generate runoff quickly and may have challenged the routing in CRHM or the ability of WRF to synthesise rainstorms. For PRLL and BRB, comparisons of the 15-WY mean daily streamflow show that model estimated slightly higher winter flow (Fig. 6f-g), likely caused by model's delay in glacier melt water. Overall, given that the model was driven with synthetic meteorology without data assimilation within the WRF domain, the results show remarkably good daily streamflow predictions for BRB and its sub-basin, the PRLL, and adequate predictions for daily streamflow for the BRLL sub-basin of the BRB and the ERC without calibration, suggesting that it can be employed to examine changes in climate in the region. It is important to realise that the CRHM model has produced very good results in this region when forced with locally observed meteorology (Fang et al., 2013; Pradhananga and Pomeroy, 2022a).

3.2. *Changes in WRF meteorology due to climate change*

The WRF near-surface meteorological variables were compared between CTL and PGW periods to show future changes in forcing climates. Fig. 7 shows mean daily time series of changes in air temperature, cumulative precipitation, relative humidity, wind speed, shortwave and longwave irradiance for the Bow and Elbow river basins, where mean annual changes shown in bold indicate they are statistically significant ($p \leq 0.05$). Seasonal changes for the same variables shown in Fig. 7 are presented in Table 3. The projections show that mean annual air temperatures will be warmer by 4.7 and 4.5 °C in the PGW period for basins of BRB and ERC, respectively (Fig. 7a-d). Spring and autumn temperatures will warm up more than the annual temperatures for both basins. In the PGW period, the dates of daily temperatures reaching 0 °C in spring will advance by 20 days for BRLL to 28 days for ERC, whilst the dates of daily temperatures dropping below 0 °C in autumn will fall 21 days later for PRLL to 29 days later for ERC. Cumulative precipitation in

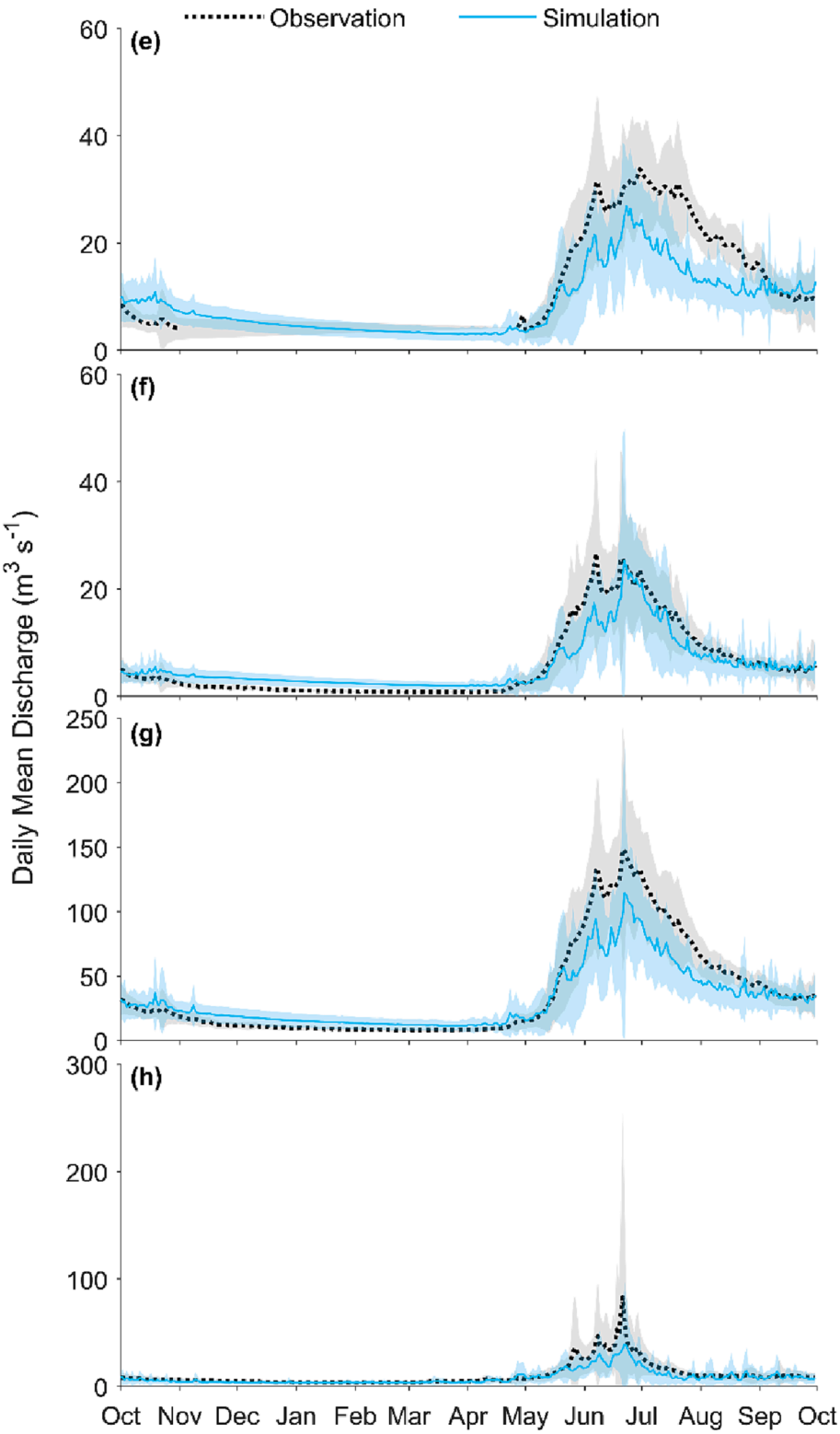

Fig. 6. (*continued*).

the PGW compared to the CTL period will increase from 87 to 149 mm or by 12–15% (Fig. 7e-h). In the BRB, more than half of the annual precipitation occur in winter under any scenario, and the largest increases in seasonal precipitation in the PGW period will also occur in winter, 110–142 mm (Table 3). For ERC, spring precipitation constitutes 45% or more of annual precipitation for any scenario and will increase by 58 mm in the PGW period. Precipitation is projected to decline by 5–25 mm and 2–11 mm respectively for summer and autumn in the PGW period for all basins (Table 3). Decreases in mean annual relative humidity in the PGW period will range from 1.2% for ERC to 3.0% for both BRLL and BRB model domains (Fig. 7i-l), with larger relative humidity decreases in spring and autumn (Table 3). Mean annual wind speed is projected to decline by 0.1 m s^{-1} in the PGW period for all basins (Fig. 7m-p), and reductions in seasonal wind speed in the PGW period will be less than

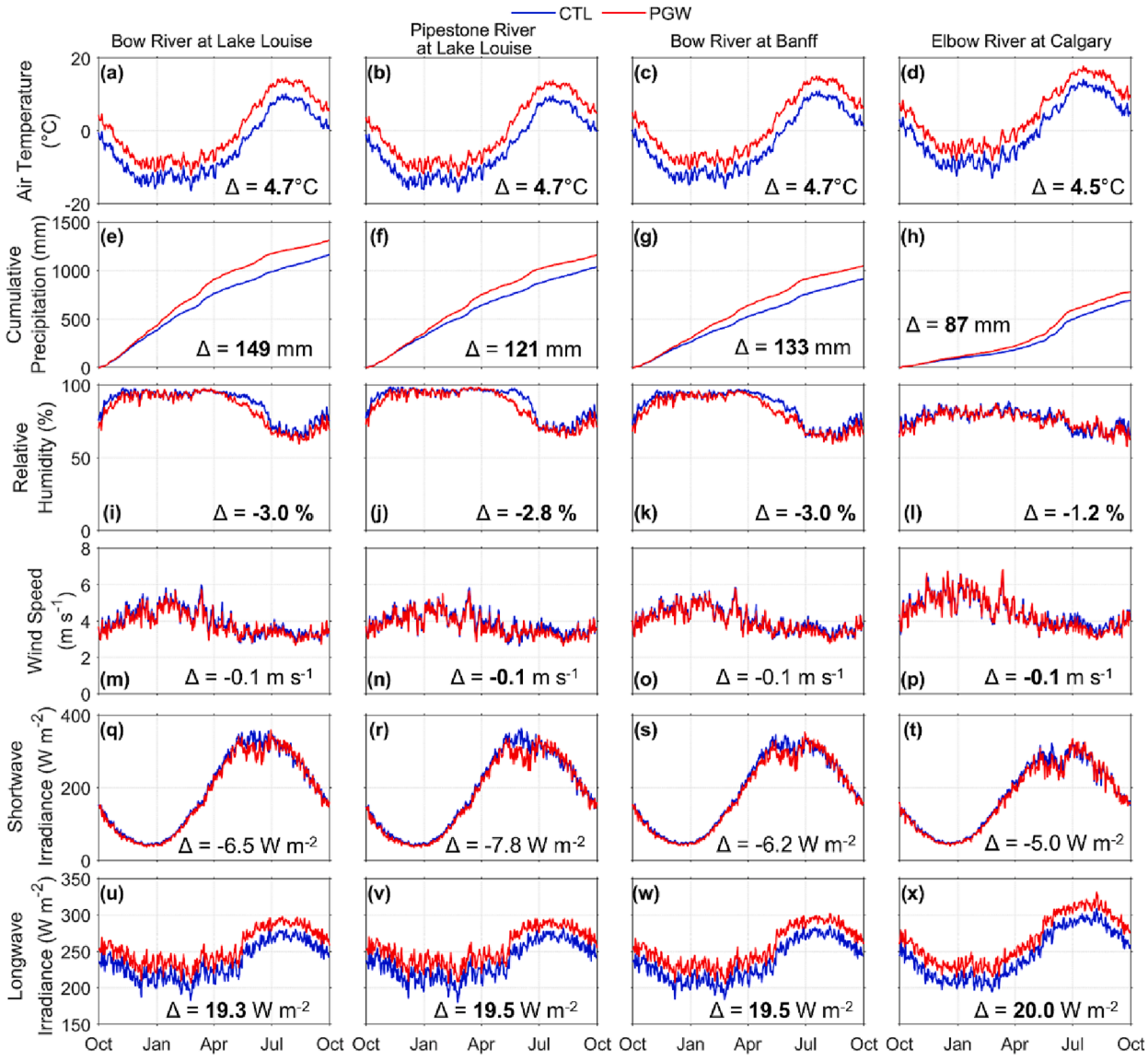

Fig. 7. Mean daily projected changes in (a-d) air temperature, (e-h) cumulative precipitation, (i-l) relative humidity, (m-p) wind speed, (q-t) shortwave irradiance, and (u-x) longwave irradiance in CTL and PGW periods for the Bow River and Elbow River basins. Mean annual change (Δ = PGW – CTL) is bold when statistically significant ($p \leq 0.05$).

Table 3
Seasonal climate changes between the CTL and PGW for the Bow and Elbow river basins.

	Winter (November to March)				Spring (April to June)				Summer (July to August)				Autumn (September to October)			
	BRLL	PRLL	BRB	ERC	BRLL	PRLL	BRB	ERC	BRLL	PRLL	BRB	ERC	BRLL	PRLL	BRB	ERC
Air temperature (°C)	4.4	4.4	4.5	4.5	5.2	5.2	5.1	4.6	4.7	4.5	4.4	4.0	5.0	5.0	4.8	4.6
Precipitation (mm)	142	110	111	37	39	37	41	58	−25	−16	−14	−5	−7	−11	−5	−2
Relative humidity (%)	−1.0	−0.9	−1.5	−1.2	−4.9	−5.2	−5.3	−1.4	−2.8	−1.7	−1.2	1.8	−5.5	−5.3	−5.2	−3.7
Wind speed (m s^{-1})	−0.2	−0.1	−0.1	0.0	−0.1	−0.1	0.0	−0.1	−0.1	−0.2	−0.2	−0.2	−0.1	−0.1	0.0	−0.1
Shortwave irradiance (W m^{-2})	−4.6	−5.8	−4.8	−4.4	−18.5	−23.1	−18.8	−13.5	4.4	6.7	6.1	4.1	−4.5	−4.5	−3.4	−3.0
Longwave irradiance (W m^{-2})	19.7	20.7	19.7	20.4	19.8	20.2	20.3	19.4	18.4	17.1	18.6	20.3	18.3	18.1	18.9	19.6

0.2 m s^{-1} (Table 3). There will be slight decreases in mean annual shortwave irradiance in the PGW period, ranging from 5.0 W m^{-2} for ERC to 7.8 W m^{-2} for PRLL (Fig. 7q-t), with noticeably higher decreases in spring and increases in summer for all basins (Table 3). Longwave irradiance will increase significantly in the PGW period for all basins, in the range between 19.3 and 20.0 W m^{-2} annually (Fig. 7u-x), with generally consistent increases in longwave irradiance throughout all seasons (Table 3).

3.3. Changes in water balance variables due to climate and concomitant glacier change

The simulated annual water balance variables for all basins were compared between the reference and climate scenario simulation, including the impact of deglaciation to show the hydrological changes predicted by the end of this century. Compared to the reference simulation, annual rainfall will increase in all basins in the climate scenario

simulation, ranging from 158 mm or 42% increase for ERC to 198 mm or 86% increase for BRLL (Fig. 8a-d). Based on the seasons defined in Table 3, rainfall will increase in winter, spring, and autumn in all basins, with the highest increases in spring, ranging from 84 mm for BRLL to 108 mm for ERC, followed by increases in winter from 26 mm for ERC to 68 mm for BRLL. For summer rainfall in the climate scenario simulation, there will be small decreases, ranging from 1 mm for ERC to 11 mm for BRLL, and no change for PRLL. Annual snowfall will decline in all basins under climate change, ranging from 49 mm or 5% decrease for BRLL to 71 mm or 22% decrease for ERC compared to the reference simulation (Fig. 8e-h). There will be seasonal snowfall decreases in spring, summer, and autumn under climate change in all basins, with the greatest

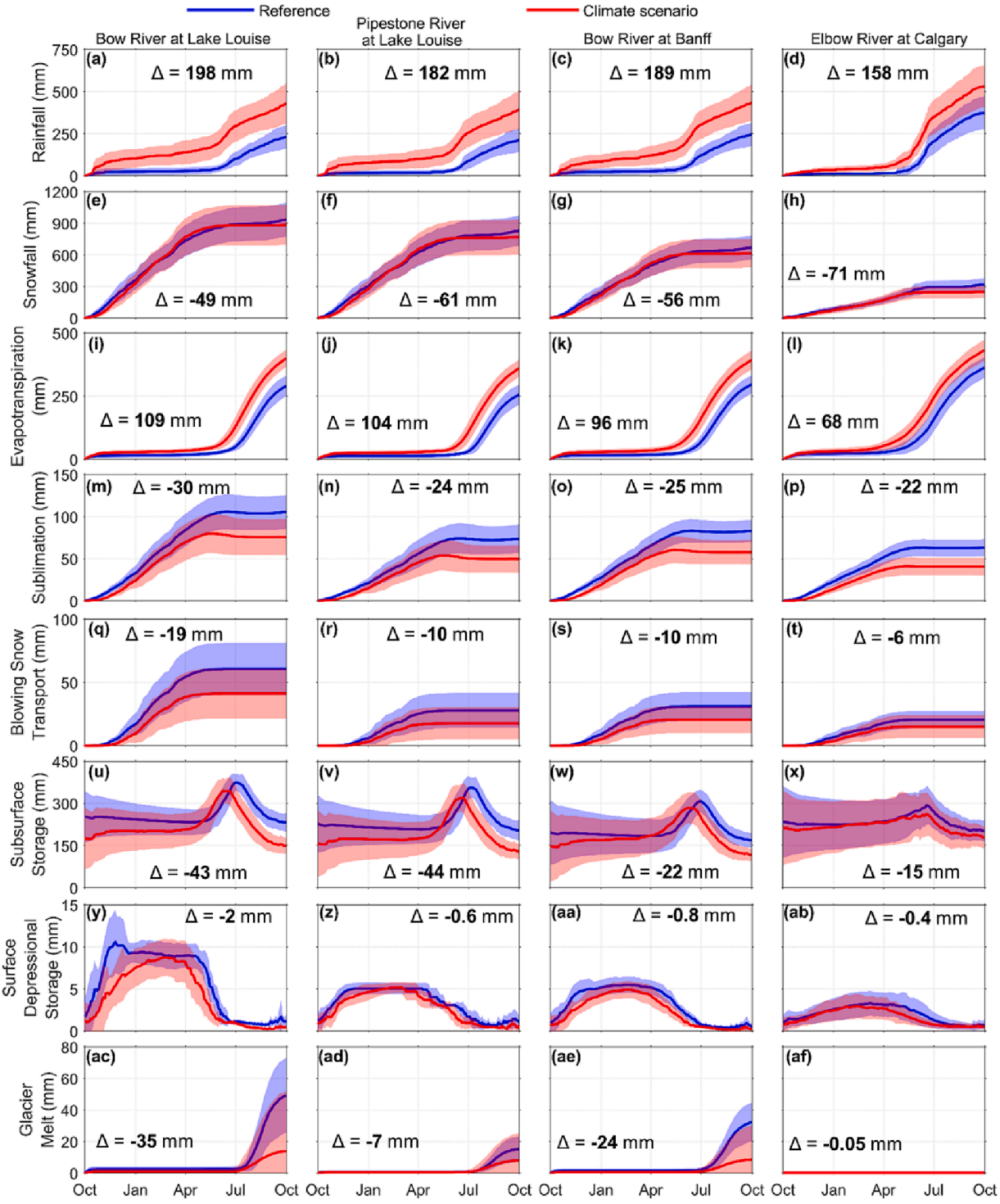

Fig. 8. Comparison of mean daily water balance variables for the Bow River and Elbow River basins between the reference and climate change simulations. (a-d) rainfall, (e-h) snowfall, (i-l) evapotranspiration, (m-p) sublimation, (q-t) blowing snow transport, (u-x) subsurface storage, (y-ab) surface depressional storage, and (ac-af) glacier melt. Variables are shown as cumulative of daily values, except for storage variables that are presented as the mean daily values. Mean annual change (Δ = Climate – Reference) is bold when statistically significant ($p \leq 0.05$). The line represents the mean and the shadow represents the standard deviation of variables over the 15 water years.

decreases in spring of from 45 to 50 mm, and in autumn ranging from 26 to 64 mm. In contrast, winter snowfall will increase under climate change in all basins, ranging from 11 mm (8%) increase for ERC to 73 mm (11%) increase for BRLL.

Evapotranspiration (ET) includes actual evaporation from soil, intercepted rain, and open water, and transpiration from plants via withdrawals of soil moisture by roots, and its annual values will be significantly higher under the climate scenario, ranging from 68 mm (+19%) for ERC to 109 mm (+38%) for BRLL (Fig. 8i-j). ET will initiate earlier in spring for all basins due to earlier snowcover depletion, ranging from 11 days for BRLL to 25 days for ERC. Sublimation includes fluxes from the surface snowpack, blowing snow and forest canopy intercepted snow, and its annual values will decrease significantly everywhere because of reduced snowfall and the effects on warmer air temperatures in suppressing blowing snow events and increasing unloading and melt (drip) of intercepted snow from forest canopies. The annual decline in sublimation will range from 22 mm (-36%) for ERC to 30 mm (-28%) for BRLL (Fig. 8m-p). Blowing snow transport is the net flux of snow redistributed by wind within a basin; it does not represent a net loss or gain of SWE from a basin, but shows the degree of snow redistribution by wind from open tundras, exposed glaciers and alpine ridgetops to lee slopes, sheltered locations including glaciers, gullies, shrubs and treeline forests. Predictions showed that the annual blowing snow transport loss will decline significantly in the future because of reduced blowing snow occurrence with rising air temperatures, wetter snowpacks, and shorter snowcovered periods, and the decreases in snow transport redistribution will range from 6 mm (-27%) for ERC to 19 mm (–32%) for BRLL (Fig. 8q-t).

Subsurface storage is the total water storage in soil and groundwater and is affected by complex interactions amongst ET, subsurface drainage, and recharges from seasonal snowmelt, glacier firnmelt and icemelt, and rainfall. Subsurface storage will rise earlier in the spring by late century, especially in the Bow River basin and its sub-basins, as result of recharge from earlier snowmelt; whilst the subsurface storage will decline in summer and autumn due to earlier and faster ET over the longer summer. Overall, the mean annual subsurface storage will decline from 23% to 19% saturation for BRLL and from 17% to 16% saturation for ERC (Fig. 8u-x). Surface storage is the total storage in lakes, stream channels, and wetlands, and its mean annual value will decline slightly under the climate scenario, with declines ranging from 0.4 mm (-18%) for ERC to 2 mm (-28%) for BRLL (Fig. 8y-ab). Glacier melt is the total melt from glacier firn and ice (does not include glacier snowmelt) and will decrease significantly in the warmer and deglaciated future (Fig. 8ac-af). Above Lake Louise, the decrease in the annual glacier melt will be 35 mm for BRLL and 7 mm for PRLL, the difference due to the higher remaining glacier coverage in BRLL, 6%, than in PRLL, 1.7%. Annual glacier melt in the BRB will decline by 24 mm, largely driven by deglaciation upstream of Lake Louise. The decrease in annual glacier melt will be very small for ERC (-0.05 mm) due to little current glacier coverage in ERC.

3.4. *Changes in snow regime due to climate and concomitant glacier change*

The simulated snow accumulation and ablation regimes for all model domains were compared between the reference and climate scenario simulation, including the impact of glacier decline on glacier snowpacks (Fig. 9), to show changes by the end of the century, where mean annual changes shown in bold indicate they are statistically significant ($p \leq 0.05$). Predictions showed that the annual peak SWE will increase in the Bow River basins, with significant increases of 3 mm (0.7%) and 30 mm (4%) in BRB and BRLL, respectively, and an increase of 21 mm (3%) in PRLL. The timing of peak SWE will advance by 18 days, from 7 May to 19 April in BRLL and PRLL and from 6 May to 18 April in BRB. The ERC snowpack will decline throughout the season, with a 20 mm (32%) decrease and one day delay, from 19 April to 20 April, in timing of peak SWE (Table 4). Future cumulative annual snowmelt volume will increase in the Bow River basin, ranging from 38 mm (5%) in PRLL to 95 mm (11%) in BRLL and 43 mm (7%) in the BRB, whilst decreasing by 55 mm (19%) in the ERC (Table 4). Similarly, the date of seasonal snowpack depletion will advance from middle/late August to late July/early August in the Bow River basin and from early July to mid-June for ERC.

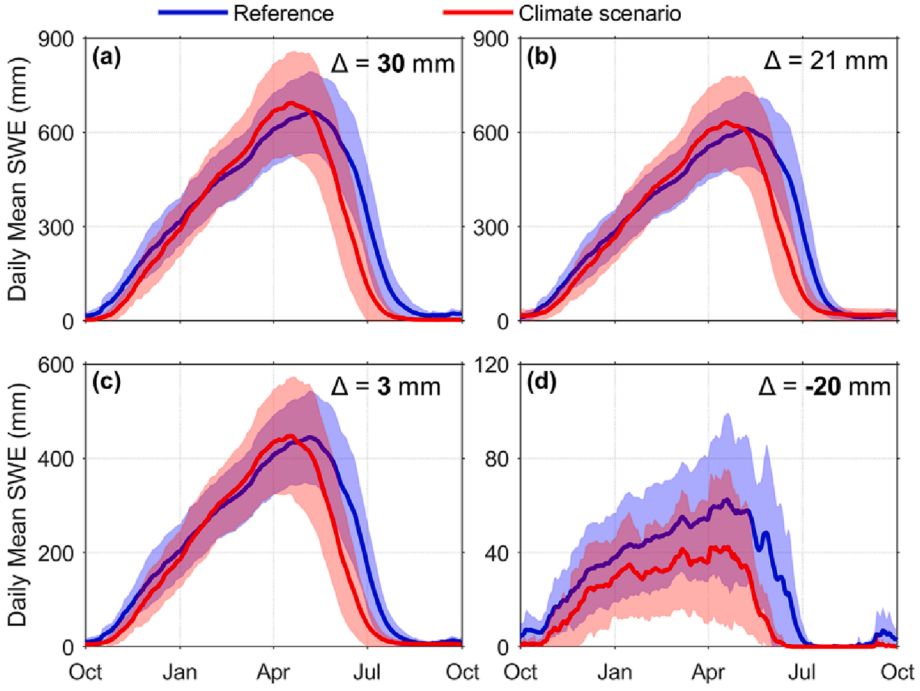

Fig. 9. Comparison of mean daily snow accumulation (SWE) for the Bow River and Elbow River basins between the reference and climate change simulations. (a) Bow River at Lake Louise, (b) Pipestone River at Lake Louise, (c) Bow River at Banff, and (d) Elbow River at Calgary. Peak SWE change (Δ = Climate – Reference) is bold when statistically significant ($p \leq 0.05$). The line represents the mean and the shadow represents the standard deviation of the 15 water year SWE.

Table 4
Snow regime changes between the reference and climate change simulations for the Bow and Elbow river basins.

	Reference				Climate Change				Difference			
	BRLL	PRLL	BRB	ERC	BRLL	PRLL	BRB	ERC	BRLL	PRLL	BRB	ERC
Cumulative snowmelt volume (mm)	867	821	648	293	962	859	691	237	95	38	43	−55
Peak SWE (mm)	664	611	444	62	694	631	447	42	30	21	3	−20
Date of Peak SWE	7 May	7 May	6 May	19 Apr	19 Apr	19 Apr	18 Apr	20 Apr	−18 days	−18 days	−18 days	1 day
Snowcover duration (day)	325	317	311	273	291	291	274	227	−34	−26	−37	−46
Melt rate (mm d^{-1})	5.9	5.9	4.5	0.8	6.5	5.9	4.7	0.8	0.6	0.0	0.2	0.0

As a result, the seasonal snowcover (converse being snow-free period) duration will decline (increase) everywhere, ranging from 26 days shorter (longer) for PRLL to 46 days shorter (longer) for ERC. The seasonal snowmelt rate was estimated by dividing the annual peak SWE by the days from peak SWE to snowpack depletion, and it will increase in the future from 4.5 mm d^{-1} to 4.7 mm d^{-1} in BRB and from 5.9 mm d^{-1} to 6.5 mm d^{-1} in BRLL, respectively. In contrast, the snowmelt rates will remain unchanged in PRLL at 5.9 mm d^{-1} and ERC at 0.8 mm d^{-1} (Table 4).

3.5. Changes in streamflow regime due to climate and concomitant glacier change

The future simulations include both climate change and glacier decline, and predict the annual peak discharge will increase for the Bow river basins but decrease for the ERC (Fig. 10a-d). Table 5 shows significant increases in the annual peak discharge ranging from 0.39 $m^3 s^{-1}$ for PRLL to 12.23 $m^3 s^{-1}$ for BRB, and a significant decrease in the annual peak discharge of 3.58 $m^3 s^{-1}$ for ERC. The timing of the annual peak discharge will advance by 15 to 17 days, from late June to early

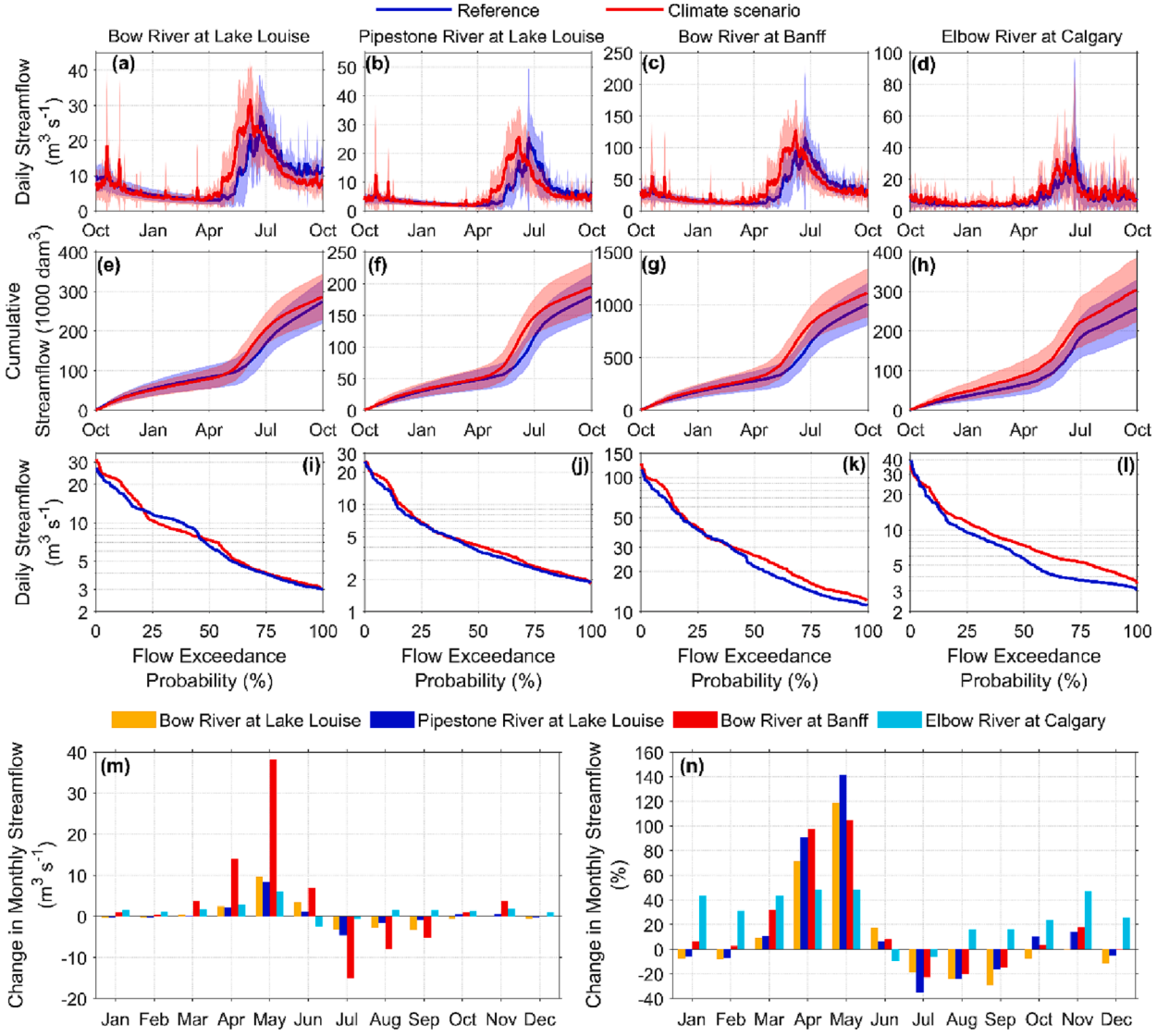

Fig. 10. Streamflow comparison for the Bow and Elbow river basins between the reference and climate change simulations over the 15 water years. (a-d) mean daily streamflow discharge, (e-h) cumulative streamflow discharge, (i-l) flow duration curve of mean daily streamflow discharge, and (m-n) change in mean monthly streamflow discharge with respect to the reference simulation. The line in (a-l) represents the mean and the shadow in (a-h) represents the standard deviation of the 15-water year streamflow.

Table 5
Streamflow regime changes between the reference and climate change simulations for the Bow and Elbow river basins. Note that peak streamflow difference (Climate – Reference) is bold when statistically significant ($p \leq 0.05$).

	BRLL	PRLL	BRB	ERC	BRLL	PRLL	BRB	ERC
	Peak streamflow discharge ($m^3 s^{-1}$)				Peak streamflow discharge difference ($m^3 s^{-1}$)			
Reference	26.94	25.28	114.44	39.59	N/A	N/A	N/A	N/A
Climate change	31.54	25.67	126.67	36.01	**4.6**	**0.39**	**12.23**	**−3.58**
	Date of peak streamflow discharge				Date of peak streamflow discharge difference			
Reference	23 Jun	22 Jun	22 Jun	22 Jun	N/A	N/A	N/A	N/A
Climate change	6 Jun	6 Jun	7 Jun	19 Jun	−17	−16	−15	−3
	D50				D50 difference			
Reference	15 Jun	17 Jun	14 Jun	8 Jun	N/A	N/A	N/A	N/A
Climate change	1 Jun	30 May	29 May	27 May	−14	−18	−16	−12

June, in the Bow river basins, and will occur three days earlier in the ERC (Table 5). The timing of onset of spring freshet will advance 38 days from early May to late March for the Bow river basins and 30 days from early April to early March for the ERC (Fig. 10a-d). The timing of the centre of flow volume (D50) will advance 14 to 18 days in the Bow river basins and 12 days in the ERC (Table 5). Annual streamflow volumes will increase by 11850, 14130, 106700, and 46,000 dam^3 for BRLL, PRLL, BRB, and ERC, respectively (Fig. 10e-h), corresponding to 4%, 8%, 11%, and 18% increases in annual water yields for Bow River at Lake Louise, Pipestone River at Lake Louise, and Bow River at Banff, and Elbow River at Calgary, respectively.

The flow duration curve (Fig. 10i-k) shows increases in daily streamflow for Bow river basins for almost all exceedance probabilities (EP) under climate scenario. For the 1% EP (return period of 100 years), daily streamflow will increase by 4.48, 1.7, and 8.78 $m^3 s^{-1}$ for BRLL, PRLL, and BRB, respectively, and for the 50% EP (return period of 2 years), daily streamflow will increase by 0.76, 0.43, and 4.55 $m^3 s^{-1}$ for BRLL, PRLL, and BRB, respectively. There will be less than 2 $m^3 s^{-1}$ decreases in daily streamflow for BRLL for the EP between 21% and 45% and for BRB for the EP between 28% and 39%. The flow duration curve (Fig. 10*l*) shows daily streamflow for Elbow River will increase for the EP greater than 4% (i.e. return period of 25 years or less) and will decrease for the EP less than 4%, with the greatest decrease of 5.65 $m^3 s^{-1}$ occurring for the 0.5% EP (return period of 200 years).

The changes in monthly streamflow discharge were calculated by subtracting the monthly discharge in climate change plus glacier decline simulation from that in the reference simulation. Fig. 10m-n shows monthly streamflow in Bow river basins will increase notably for April to June, with the greatest increases in May, ranging from 8.42 $m^3 s^{-1}$ (+142%) for PRLL to 38.28 $m^3 s^{-1}$ (+105%) for BRB. Monthly streamflows will decrease in Bow river basins for July to September, with the greater decreases in July, ranging from 3.28 $m^3 s^{-1}$ (-19%) for BRLL to 14.97 $m^3 s^{-1}$ (–23%) for BRB. For autumn and winter months, changes in monthly streamflow will be mixed in Bow river sub-basins, with monthly streamflow in BRLL varying from a 0.7 $m^3 s^{-1}$ decrease in October to a 0.31 $m^3 s^{-1}$ increase in March and for PRLL ranging from a 0.16 $m^3 s^{-1}$ decrease in January and February to a 0.51 $m^3 s^{-1}$ increase in November. In contrast, monthly streamflows will mostly increase in BRB during autumn and winter months, ranging from 0.33 $m^3 s^{-1}$ in February to 3.74 $m^3 s^{-1}$ in November, except for 0.08 $m^3 s^{-1}$ decrease in

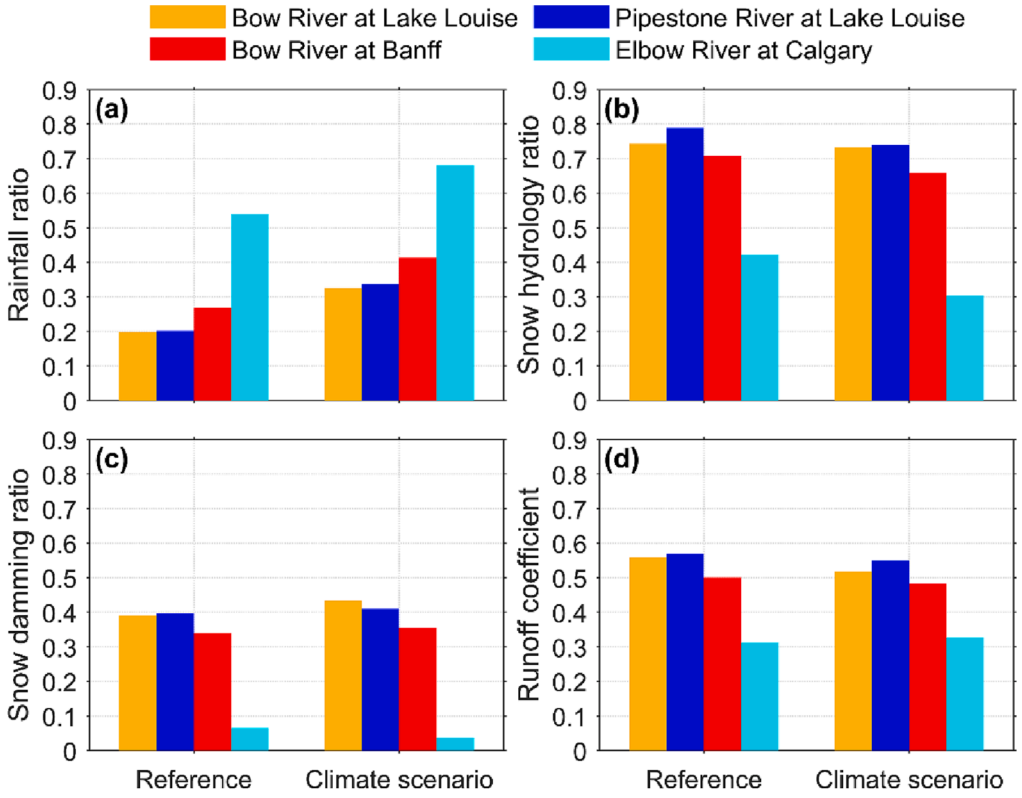

Fig. 11. Comparison of streamflow regime indices for the Bow and Elbow river basins between the reference and climate change simulations. (a) Rainfall ratio, (b) snow hydrology ratio, (c) snow damming ratio, and (d) runoff coefficient.

December. For the Elbow River, monthly streamflow will increase for all months except for June and July, ranging from increases of 0.93 $m^3 s^{-1}$ (26%) in December to 6.07 $m^3 s^{-1}$ (48%) in May, contrasted with 2.45 $m^3 s^{-1}$ (9%) and 0.7 $m^3 s^{-1}$ (6%) decreases respectively in June and July.

Fig. 11 shows the comparison of 15-WY mean values for the hydrological indices between the reference and climate change plus glacier decline simulations for each basin. The RR will increase from 0.2 to 0.33 for BRLL and 0.34 for PRLL and will rise from 0.27 to 0.41 for the BRB as a whole. Bow river basins will remain snowfall-dominated despite the increasing RR, but not the Elbow River where the RR will increase from 0.54 to 0.68. The SHR will decrease by 0.01, 0.05, and 0.05 to 0.73, 0.74, and 0.66 for BRLL, PRLL, and BRB, respectively, suggesting that snow hydrology will remain the overwhelmingly dominant runoff mechanism in the upper Bow River above Lake Louise and will remain important for the Bow River at Banff. For the Elbow River, the SHR will decline from 0.42 to 0.3, indicating that rainfall-runoff will become more dominant and snow hydrology less important by late century. The SDR will increase by 0.04, 0.01 and 0.02 to 0.43, 0.41, and 0.36 for BRLL, PRLL, and BRB, respectively, suggesting that snowpack's storage as natural water reservoir will rise slightly for Bow river basins. For the Elbow River, the SDR is currently low, 0.06, and will decline to 0.04, indicating a very low snowpack storage capacity. The RC will decrease by 0.04, 0.02 and 0.02 to 0.52, 0.55, and 0.48 for BRLL, PRLL, and BRB, respectively, suggesting a future decline in streamflow generation efficiency for Bow river basins. For Elbow River, the RC will increase by 0.02 to 0.33, but streamflow generation efficiency will remain low.

3.6. Glacier falsification

In Falsification 1 (i.e. WRF CTL climate with a diminished RCP8.5 projected glacier coverage), annual streamflow volume declines by 24400, 1130, and 36,960 dam^3 for BRLL, PRLL, and BRB, respectively compared to the reference simulation (Fig. 12a-c). The reduced streamflow volume can be completely attributed to the 99% decrease in glacier ice volume projected by RCP8.5, in this case running with the WRF CTL climate. This falsification estimates a current glacier wastage contribution of 8.9%, 0.6%, and 3.7% of annual streamflow for Bow River at Lake Louise, Pipestone River at Lake Louise, and Bow River at Banff, respectively. For ERC, there was a minimal decrease (i.e. 10 dam^3) in annual streamflow volume with glacier removal from the basin (Fig. 12d), suggesting a negligible current glacier wastage contribution to the flow of the Elbow River at Calgary.

In Falsification 2 (i.e. WRF PGW climate with the current RGI 3.2 glacier coverage), the annual glacier ice and firn melt will increase by 90 mm (184%), 42 mm (274%), and 52 mm (163%) for BRLL, PRLL, and BRB (Fig. 12e-g), indicating significantly higher annual glacier wastage contributions to the Bow river basins if the future climate also had the current RGI 3.2 glacier coverage. In contrast, the increase in glacier wastage for this falsification was very small (0.05 mm) for ERC as result of its very limited current glacier coverage (Fig. 12h).

4. Discussion

Uncalibrated hydrological simulations forced by WRF near-surface meteorological variables at 4 km during 2000–2015 can make reasonable and useful predictions of seasonal snow accumulation, snowmelt, and streamflow for headwater river basins in Canadian Rockies compared to field observations. This is encouraging given the complex mountain terrain, high heterogeneity of land cover and uncertainty in initial and boundary conditions in these basins. The 4-km WRF near-surface meteorological variables were found to be biased when compared to detailed weather station observations from a small, well-instrumented mountain research basin near to the BRB and ERB, and bias correction by downscaling these 4 km WRF variables to observations improved hydrological simulations with a similar CRHM model (Fang and Pomeroy, 2020). However, observations are very sparse in the BRB and ERC, especially at high elevations, and this restricted opportunities to correct for WRF biases in this study, thus these WRF variables, especially precipitation, without bias correction can cause the model unable to capture the extreme events such as the 2005 and 2013 floods and 2008 and 2011 high flows in the ERC. Earlier modelling studies of the Bow River headwaters have forced models either using sparse weather station observations (Farjad et al., 2016) or coarse-resolution numerical weather prediction outputs that were bias-corrected to a single climate station (Gobena and Gan, 2010). The sparse or coarse-resolution forcing data was not able to fully resolve mountain topography and models were heavily calibrated to streamflow, which may have also compensated for errors in the forcing data, thereby introducing an unacknowledged uncertainty in applying these models for assessing future mountain hydrology from climate change. The uncalibrated approach with dynamically downscaled climate model forcings used here makes differences between predictions and observations fully apparent and does not attempt to compensate for biases in forcing

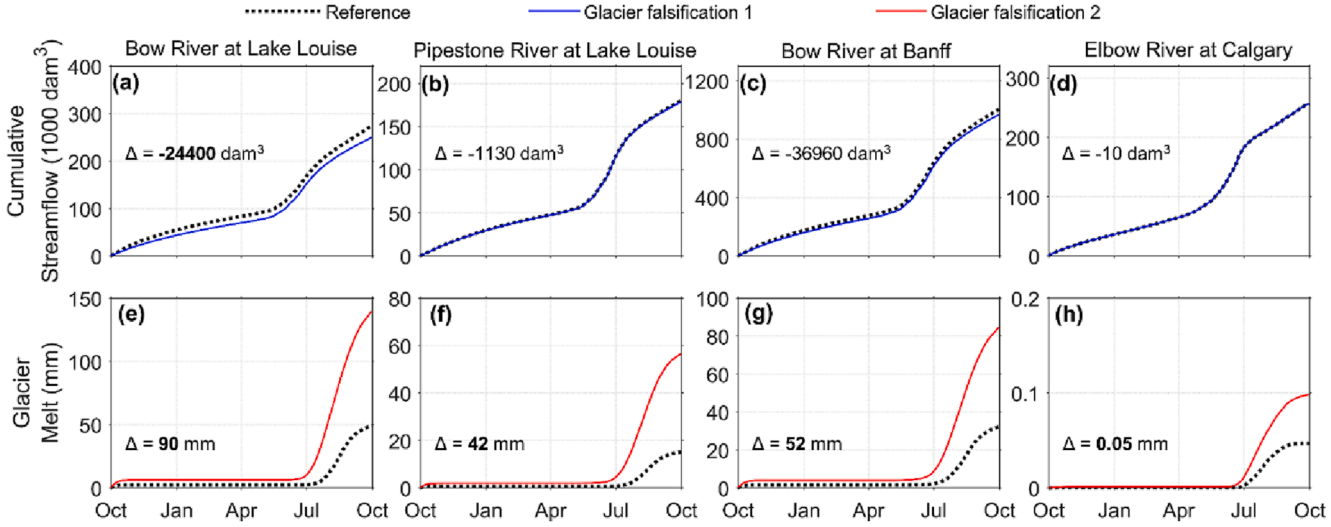

Fig. 12. Comparison of mean cumulative streamflow and glacier melt for the Bow and Elbow river basins over 15 water years between the reference and (a-d) cumulative streamflow from glacier Falsification 1 (i.e. WRF CTL climate and RCP8.5 projected glacier), (e-h) cumulative glacier melt from glacier Falsification 2 (i.e. WRF PGW climate and current RGI 3.2 glacier). Mean annual change (Δ = Falsification – Reference) is bold when statistically significant ($p \leq 0.05$).

meteorology, thereby providing a more certain hydrological response to the dynamics of future climate, with known model deficiencies.

Uncalibrated hydrological modelling using CRHM can reproduce the seasonality of the observed streamflow for the Bow River headwater basins, reflecting operation of the physically based routines for snow accumulation, redistribution and melt. However, the model does have some deficiency in simulating streamflow for the Bow River at Lake Louise that contains higher glacier coverage, likely attributed to the general representation of routing for glaciers, in that firn and ice melt is routed through linear reservoirs represented by firn and ice storage before being released to and routed through the subsurface and groundwater. Subsequently, the slower routed glacier melt water to streamflow resulted in slightly higher winter flow for Bow River at Banff compared to the observation. Recent hydrological modelling using CRHM showed good streamflow predictions for Peyto and Athabasca glacier basins in the Canadian Rockies (Aubry-Wake and Pomeroy, in review; Pradhananga and Pomeroy, 2022b), suggesting that streamflow simulation for glaciers can be improved with more specific routing sequence for individual glaciers. In addition, the flashness in streamflow simulation for Elbow River, especially the rainfall-generated streamflow, reflects some challenges in routing flow in narrow mountain valleys and in representing large and complex foothills and agricultural regions with a relatively few numbers of HRUs. These limitations limit model performance and because it is uncalibrated are very apparent when examining synthesized streamflows in comparison to measured ones.

As the Bow River headwater basins contain large variations in elevation, aspect and slope and high heterogeneity of land cover, the model considers different HRUs based on criteria of elevation, slope and aspect for glacier, alpine rock and tundra as well as land cover types. This model complexity is decided upon using the deductive and abductive reasoning approach described by Pomeroy et al. (2013). That is, the deductive reasoning utilizes known physical laws and relationships to derive information from existing basin inventories and applies rule-based continuity equations for predictions, while abductive reasoning emphasizes the inference of information from research basins in the region. This study avoids the inductive reasoning when deciding model complexity, as such approach replies on calibration of current observations that can shift in the future climate and would be biased due to the synthetic meteorology used to force the model. Since the optimal model complexity is likely to change in a warming cold region such as the Canadian Rockies, this model's spatial and process complexity was felt to be important to permit robust simulations and physical process diagnosis of future changes in mountain hydrology.

The basins of the Bow River at Banff and Elbow River at Calgary will warm up significantly, by 4.7 and 4.5 °C, and will receive 12% to 15% more precipitation annually under the business-as-usual climate change scenario (RCP8.5); the warmer and wetter future climates are similar to other findings for the late 21st century found in this region (Fang and Pomeroy, 2020; Kienzle et al., 2012). Under climate change, annual precipitation will transition towards more rainfall and less snowfall for all basins, with the Bow river basins remaining snowfall-dominated whilst the Elbow River will become a rainfall-dominated regime. For all basins, rainfall will increase for all seasons except for summer when overall precipitation will decline, in contrast, snowfall will decrease for all seasons except for winter. For both historical and future climates, winter precipitation accounts for 50% or more of annual precipitation for the Bow River basins, whilst spring precipitation contributes at least 45% of annual precipitation in Elbow River at Calgary. This is associated with the difference in seasonal weather patterns between the Bow River and Elbow River basins (Thériault et al., 2015; Wood et al., 2018). Pacific air masses produce storms that cross the continental divide from the west and precipitate over the Central ranges of Canadian Rockies in winter, whilst continental air masses generate infrequent but large upslope storms coming from the east and precipitating over the Front Ranges of Canadian Rockies in spring. Under climate change, both the Bow River and Elbow River basins will experience reduced blowing snow transport, diminished sublimation losses from blowing snow in the alpine and intercepted snow in forests, shorter snowcovered periods and earlier snow depletion. These changes are consistent with snow process-based modelling results for warmer and wetter climates in Canadian Rockies Front Ranges (Fang and Pomeroy, 2020; Lapp et al., 2005; Pomeroy et al., 2015; Rasouli et al., 2022; Tanzeeba and Gan, 2012), Central Ranges (Aubry-Wake and Pomeroy, in review) and other high mountain basins (López-Moreno et al., 2013, 2020; Marty et al., 2017). The decline in snowpacks throughout the season in the Elbow River Basin under the climate scenario appear to be influenced by warmer Chinook events, which develop frequently in the Front Ranges and foothills of Canadian Rockies and result in snowcover depletion from rapid melt and sublimation (MacDonald et al., 2018). In contrast, the higher peak snow accumulation and melt volumes under climate change in the Bow River basins will result from the winter maximum in seasonal precipitation increases predicted for these basins. The results also caused mixed responses in snowmelt rates under climate change, with slightly higher melt rates for the Bow River at Banff but unchanged rates for Elbow River at Calgary, which both contrast with predictions of slower snowmelt rates in a warmer climate for this region (Musselman et al., 2017). The Bow River headwaters contain a range of ecozones that span a large elevational gradient, and the response of snowmelt rates to climate change varies in these ecozones due to the complex interplay amongst changes in air temperature, precipitation, snow redistribution, albedo decay, and seasonal variation in radiation fluxes to snowpack (Fang and Pomeroy, 2020; Lopez-Moreno et al., 2020).

This study assessed the glacier contributions to streamflow in Bow River headwaters based on a comparison of simulated mean annual streamflow volumes between hydrological models with current glacier coverage and a falsification consisting of a 99% reduction in glacier coverage for the same climate. This is the same modelling approach for investigating glacier contribution to streamflow in Bow River above Lake Louise employed by Naz et al. (2014) and for the Peyto and Athabasca glacier basins (Pradhananga and Pomeroy, 2022b). For the Bow River at Banff, the 3.7% glacier (ice plus firn melt) contribution to mean annual streamflow during 2000–2015 from this study is lower than the 4.9% during 2000–2009 estimated by Bash and Marshall (2014) and is higher than the 1.98% estimated during 1952–1993 by Hopkinson and Young (1998), the 2.2% during 1975–1998 by Comeau et al. (2009), and the 2.8% during 1976–1998 by Demuth et al. (2008). These differences result from the different initial glacier coverage, interannual variabilities in streamflow and glacier wastage during these different periods (Bash and Marshall, 2014; Demuth et al., 2008), glacial retreat influence on glacial wastage (Naz et al., 2014) and differences in melt calculation methodologies which range from temperature index estimates to energy balance melt models and various forcing meteorologies and scales.

As a result of shorter snowcover duration and earlier depletion under climate change, the onset of the spring snowmelt freshet advanced from May to late March for the Bow river basins and to early March for Elbow River. Streamflow declined during July and August for Bow river basins and during June and July for Elbow River under climate change because of higher evapotranspiration loss, reduced redistribution of snow causing faster snowpack depletion, earlier meltwater availability, and reduced alpine summer snowmelt and glacier melt. The impact later in summer in the Bow River is because of its greater glacier melt contribution and one-month longer persistence of snowpacks. The shift in spring snowmelt freshet and decline in summer streamflow with climate change have been found for many snow-dominated basins in Canadian Rockies (Fang and Pomeroy, 2020; Islam and Gan, 2015; Kienzle et al., 2012; Rood et al., 2008) and glacier melt dominated basins where climate change is accompanied by deglaciation (Aubry-Wake, 2022). The annual peak discharge under climate change increased for the Bow River basins but decreased for the Elbow River; this is due to the Bow River basins being much more dominated by snow hydrology, and

having higher seasonal peak snowpacks and snow damming ratios for storing water to feed the spring freshet compared to the Elbow River Basin. Nevertheless, both basins will have substantial increases in annual discharge volumes, 11% for Bow River at Banff and 18% for the Elbow River at Calgary, under climate change. The increase in annual streamflow volume with climate change for the Elbow River is very comparable to values found for other Canadian Rockies basins (Fang and Pomeroy, 2020; Kienzle et al., 2012), whilst the smaller increase for the Bow River is attributed to diminished glacier contributions to streamflow under climate change. For the two upper Bow River basins, the projected 4% increase in annual streamflow for Bow River at Lake Louise is lower than 8% increase for the Pipestone River at Lake Louise. This reflects the reduced glacier contribution to streamflow suppressing the effect of higher precipitation in the high mountain, partly glaciated and lake dominated basin of the Bow River above Lake Louise compared to steep, sparsely glaciated, high mountain environments of the Pipestone River Basin.

The projected increases in streamflow for Bow River headwaters contrast with earlier studies indicating declines in streamflow for this region in the 21st century (Farjad et al., 2016; Islam and Gan, 2015). Decreasing streamflow from these earlier studies is attributed to coarse GCM/RCM scale forcing data that have high degree of uncertainty and a large inter-model variability in future precipitation for the Canadian Rockies. Low resolution climate models cannot reliably predict high mountain precipitation and convective storms in mountains that are important in governing the hydrology of the eastern slopes of the Canadian Rockies. The dynamically downscaled climate change scenario and forcing data from WRF-PGW for this study is felt to be an improvement on previous studies in the region that used statistically downscaled RCMs or GCMs that could not directly resolve mountain meteorology and precipitation processes. WRF-PGW is bounded by results from a 19-model RCM-GCM ensemble mean change imposed on ERA-Interim forcing, permits explicit convective storm microphysics representation and can resolve sharp mountain topography and orography with its 4-km resolution. This study took advantage of the WRF-PGW approach by running hydrological simulations with the 19-model ensemble mean change instead of each RCM-GCM projection to avoid large uncertainties resulted from inter-model variability. Limitations of this dynamically downscaled approach include the lack of multiple representations of future climate to permit assessment of forcing uncertainty, introducing imbalances to lateral boundary forcing by adding nonlinear terms in climate change signal, and the inability to track future storms and estimate the changes in future storm frequency and intensity as a result of non-representation of nonlinear interactions between atmospheric circulation changes and climate warming (Li et al., 2019). The research of Gizaw and Gan (2016) and Sillmann et al. (2013) has suggested that more frequent and intensive storm events in spring and summer are expected for the Canadian Rockies in late 21st century, which could lead to a higher risk of future flooding. WRF-PGW can represent how past atmospheric dynamics will play out in a warmer, wetter atmosphere, but not these new atmospheric dynamics and thus caution should be taken in interpreting the results for peak annual flows.

This study examined the hydrological impact of climate change from the worst-case high emission scenario represented by the "business-as-usual" RCP8.5 scenario, while there are other emission scenarios such as low emission (RCP2.6) and medium emission (RCP4.5) scenarios. The projected median changes for 2081–2100 relative to 1986–2005 based on CMIP5 multi-model ensemble include annual mean air temperature warming by 1.7 °C in RCP2.6 and 2.9 °C in RCP4.5 and annual precipitation increasing by 6.8% in RCP2.6 and 9.2% in RCP4.5 for Alberta (Environment and Climate Change Canada, 2023). Assessing the hydrological impact of these low to medium emission scenarios is recommended for the future study to explore the uncertainties among these climate change scenarios, and some caution should be taken when interpreting this study's results using the RCP8.5 scenario. In addition, the 99% reduction in the glacier ice volume under the RCP8.5 climate change scenario was guided by a RCP8.5 deglaciation projection value of glacier volume for the southern Canadian Rockies (Clarke et al., 2015). This RCP8.5 deglaciation projection is based on multi-model GCM ensemble mean and has uncertainties in GCM future climate projections, ice dynamics modelling and the surface mass balance model, especially its empirical melt parameters. These uncertainties could affect the future glacier extent projection and should be borne in mind when interpreting the results.

The results also suggest earlier snowmelt recharge of subsurface moisture in spring and lower subsurface moisture storage throughout the summer as a result of reduced snow redistribution, earlier and faster snowmelt, higher evapotranspiration and lower late summer precipitation under climate change. This could prolong the fire season (Morgan et al., 2008; Westerling et al., 2006) and increase risk of forest fire in this region (Macias Fauria and Johnson, 2008; Mori and Johnson, 2013). The projected warmer winter air temperature under climate change could develop favourable conditions for mountain pine beetle infestation and other forest diseases (Aukema et al., 2008; Woods et al., 2005). Impacts of forest disturbances (Pomeroy et al., 2012) and effects of combined climate, forest, and soil changes (Rasouli et al., 2019b) on hydrological processes have been examined for Marmot Creek, a small Canadian Rockies headwater basin. Such studies of combined climate, glacier, forest, and soil changes on hydrological processes and basin response are needed for the larger Canadian Rockies-sourced river basins to see how the combined impacts scale up to larger river basins and to better inform water resources and forest management adaptation to climate change.

5. Conclusions

This study developed physically based hydrological models using the CRHM platform that were forced with 4-km WRF near-surface meteorology outputs in CTL (i.e. 1 October 2000 to 30 September 2015) with current glacier coverage and pseudo global warming (PGW, i.e. 1 October 2084 to 30 September 2099) with Representative Concentration Pathway 8.5 (RCP8.5) projected glacier coverage to diagnose the future changes in hydrology caused by the concomitant climate and glacier changes in several Bow River headwater basins. Model evaluations using the observed snow accumulation and streamflow showed that the model is able to provide reasonable predictions of snow accumulation, snowmelt, and streamflow for these basins, except for adequate streamflow predictions for Bow River at Lake Louise and Elbow River. Under the business-as-usual climate change (RCP 8.5) represented by the PGW period, the basins of the Bow River at Banff and Elbow River at Calgary will warm by 4.7 and 4.5 °C, respectively, and receive 12% to 15% more precipitation annually, with both basins experiencing a greater proportion of precipitation as rainfall. As a result, increases in annual rainfall ranging from 158 mm (+42%) for basins of the Elbow River at Calgary to 198 mm (+86%) for the Bow River at Lake Louise and decreases in annual snowfall ranging from 49 mm (-5%) for the basins of the Bow River at Lake Louise to 71 mm (–22%) for the Elbow River at Calgary will occur. The high mountain winter snowfall will increase by from 11 mm (8%) for basins of the Elbow River at Calgary to 73 mm (11%) for the Bow River at Lake Louise, despite the decline in spring and summer snowfall. Hydrological processes will have complex responses to the future climate, including annual ET increases ranging from 68 mm (+19%) for basins of the Elbow River at Calgary to 109 mm (+38%) for the Bow River at Lake Louise, lower annual sublimation, ranging from 22 mm (-36%) for basins of the Elbow River at Calgary to 30 mm (-28%) for the Bow River at Lake Louise, slightly lower annual mean subsurface moisture content, but greater soil drying in late summer, and surface storage in lakes, stream channels, and wetlands decreasing by 0.4 mm (-18%) for basins of the Elbow River at Calgary to 2 mm (-28%) for the Bow River at Lake Louise. Common snow regime changes under the climate change between the basins of Bow River and Elbow River will include earlier snowcover depletion and substantially shorter snowcover duration, with declines ranging from 26 days for the basins of the

Pipestone River at Lake Louise to 46 days for the Elbow River at Calgary. Sublimation losses from blowing snow transport and snow interception will decline substantially in all basins due to warmer winters suppressing blowing snow transport and increasing unloading of snow from forest canopies. Contrasting snow regime changes will include an increasing annual peak SWE from 3 mm (+0.7%) for basins of the Bow River at Banff to 30 mm (+4%) for the Bow River at Lake Louise, higher annual snowmelt volume from 38 mm (+5%) for the Pipestone River at Lake Louise to 95 mm (+11%) for the Bow River at Lake Louise, contrasting with 20 mm (–32%) lower peak SWE and 55 mm (-19%) less snowmelt volume for the basin of the Elbow River at Calgary. Snowmelt rates will increase or remain unchanged, ranging from 0.2 mm d^{-1} faster snowmelt rates for the basin of the Bow River at Banff and no change in melt rate for the Elbow River at Calgary. The faster areal snowmelt is due, in part, to reduced snow redistribution from suppression of blowing snow and snow interception processes in warmer winters. Annual peak discharge for the Bow River at Banff under climate change will increase by 12.23 m^3 s^{-1} and its timing will advance by 15 days, with an 11% higher annual water yield. Despite the increase in annual water yield, there will be a slight decline in streamflow generation efficiency for the Bow River at Banff due to the loss of most glacier contributions to streamflow under climate change by late 21st century. In contrast, peak discharge will decrease by 3.58 m^3 s^{-1} and occur 3 days earlier, with 18% greater annual water yield in the Elbow River at Calgary under climate change. Despite a slight increase in the runoff coefficient under climate change, the Elbow River at Calgary will remain a relatively low water yield basin due to its reliance on rainfall-runoff to support streamflow.

CRediT authorship contribution statement

Xing Fang: Conceptualization, Data curation, Formal analysis, Investigation, Methodology, Software, Validation, Visualization, Writing – original draft, Writing – review & editing. **John W. Pomeroy:** Conceptualization, Formal analysis, Investigation, Methodology, Supervision, Writing – review & editing.

Declaration of Competing Interest

The authors declare that they have no known competing financial interests or personal relationships that could have appeared to influence the work reported in this paper.

Data availability

In addition to supplementary data in Appendix A, other data will be made available on request.

Acknowledgements

The authors would like to gratefully acknowledge funding support from the Canada First Research Excellence Fund's Global Water Futures programme, Alberta Government departments of Environment and Parks, and Agriculture and Forestry; Alberta Innovates; Environment and Climate Change Canada; the Natural Sciences and Engineering Research Council of Canada's Discovery Grants and Changing Cold Regions Network, the University of Saskatchewan Global Institute for Water Security, and the Canada Research Chairs programme.

Appendix A. Supplementary data

The model simulated daily streamflow for four test basins can be found in "Supplement_Model simulated daily discharge.csv". Supplementary data to this article can be found online at https://doi.org/10.1016/j.jhydrol.2023.129566.

References

Adam, J.C., Hamlet, A.F., Lettenmaier, D.P., 2009. Implications of global climate change for snowmelt hydrology in the twenty-first century. Hydrol. Process. 23, 962–972. https://doi.org/10.1002/hyp.7201.

Alberta Agriculture and Forestry, 2018. Alberta Vegetation Inventory Extended attributes (AVIE) inventory. Alberta Agriculture and Forestry, Forest Management Branch, Edmonton, Alberta.

Alberta Environment and Sustainable Resource Development, 2012. Watercourses (1: 20,000) polylines and Waterbodies (1:20,000) polygons digital data. Data Management Section, Data, Monitoring and Validation Branch, Monitoring and Science Division, Edmonton, Alberta.

Armstrong, R.N., 2011. Spatial variability of actual evaporation in a prairie landscape. Department of Geography & Planning, University of Saskatchewan, Saskatoon, Saskatchewan, Canada, p. 194. Unpublished Ph.D. thesis,.

Ashmore, P., Church, M., 2001. The impact of climate change on rivers and river processes in Canada. Geological Survey of Canada, Bulletin 555, Natural Resources of Canada, Ottawa, pp. 58. https://doi.org/10.4095/211891.

Aubry-Wake, C., 2022. From Processes to Predictions in Hydrological Modelling of Glacierized Basins. Department of Geography & Planning, University of Saskatchewan, Saskatoon, p. 281 p.. Unpublished PhD thesis,.

Aubry-Wake, C., Pomeroy, J.W., n.d. Predicting hydrological change in an alpine glacierized basin and its sensitivity to landscape evolution and meteorological forcings. Water Resour. Res. in review.

Aubry-Wake, C., Pradhananga, D., Pomeroy, J.W., 2022. Hydrological process controls on streamflow variability in a glacierized headwater basin. Hydrol. Process. 36, e14731.

Aukema, B.H., Carroll, A.L., Zheng, Y., Zhu, J., Raffa, K.F., Moore, R.D., Stahl, K., Taylor, S.W., 2008. Movement of outbreak populations of mountain pine beetle: influence of spatiotemporal patterns and climate. Ecography 31, 348–358.

Ayers, H.D., 1959. Influence of soil profile and vegetation characteristics on net rainfall supply to runoff. Proceedings of Hydrology Symposium No.1: Spillway Design Floods, NRCC, Ottawa, 198-205.

Bash, E.A., Marshall, S.J., 2014. Estimation of glacial melt contributions to the Bow River, Alberta, Canada, using a radiation-temperature melt model. Ann. Glaciol. 55 (66), 138–152. https://doi.org/10.3189/2014AoG66A226.

Bayrock, L.A., Reimchen, T.H., 1980. Surficial geology of the Alberta Foothills and Rocky Mountains, Alberta Geological Survey, Map 150. Alberta Research Council, Edmonton, Alberta.

Beke, G.J., 1969. Soils of three experimental watersheds in Alberta and their hydrological significance. Department of Soil Science, University of Alberta, Edmonton, p. 456. Ph.D. thesis,.

Beniston, M., 2005. Mountain climates and climatic change: an overview of processes focusing on the European Alps. Pure Appl. Geophys. 162, 1587-1606. https://doi.org/ 10.1007/s00024-005-2684-9.

Bernhardt, M., Schulz, K., 2010. SnowSlide: a simple routine for calculation gravitational snow transport. Geophys. Res. Let. 37 (11), L11502. https://doi.org/10.1029/2010GL043086.

Bolch, T., Menounos, B., Wheate, R., 2010. Landsat-based inventory of glaciers in western Canada, 1985–2005. Remote Sens. Environ. 114 (1), 127–137.

Burn, D.H., Abdul, Aziz, O.I., Pietroniro, A., 2004. A comparison of trends in hydrological variables for two watersheds in the Mackenzie River Basin. Can. Water Resour. J. 29 (4), 283–298.

Castilla, G., Hird, J., Hall, R.J., Schieck, J., McDermid, G.J., 2014. Completion and updating of a Landsat-based land cover polygon layer for Alberta, Canada. Can. J. Remote Sens. 40 (2), 92–109. https://doi.org/10.1080/07038992.2014.933073.

Chow, V.T., 1959. Open Channel Hydraulics. McGraw-Hill Inc, New York.

Chow, V.T., 1964. Handbook of Applied Hydrology. McGraw-Hill Inc, New York.

Clark, C.O., 1945. Storage and the unit hydrograph. Proc. Am. Soc. Civil Eng. 110 (1), 1419–1446.

Clarke, G.K.C., Anslow, F.S., Jarosch, A.H., Radić, V., Menounos, B., Bolch, T., Berthier, E., 2013. Ice volume and subglacial topophraphy for Western Canadian glaciers from mass balance fields, thinning rates, and a bed stress model. J. Climate 26, 4282–4303.

Clarke, G.K.C., Jarosch, A.H., Anslow, F.S., Radić, V., Menounos, B., 2015. Projected deglaciation of western Canada in the twenty-first century. Nat. Geosci. 8, 372–377. https://doi.org/10.1038/ngeo2407.

Comeau, L.E.L., Pietroniro, A., Demuth, M.N., 2009. Glacier contribution to the North and South Saskatchewan Rivers. Hydrol. Process. 23, 2640–2653. https://doi.org/10.1002/hyp.7409.

Conway, J.P., Pomeroy, J.W., Helgason, W.D., Kinar, N.J., Challenges in modeling turbulent heat fluxes to snowpacks in forest clearings. J. Hydrometeorol., 19, 1599-1616. https://doi.org/10.1175/JHM-D-18-0050.1.

DeBeer, C.M., Pomeroy, J.W., 2010. Simulation of the snowmelt runoff contributing area in a small alpine basin. Hydrol. Earth Syst. Sci. 14, 1205–1219. https://doi.org/10.5194/hess-14-1205-2010.

DeBeer, C.M., Pomeroy, J.W., 2017. Influence of snowpack and melt energy heterogeneity on snow cover depletion and snowmelt runoff simulation in a cold mountain environment. J. Hydrol. 553, 199–213. https://doi.org/10.1016/j.jhydrol.2017.07.051.

DeBeer, C.M., Wheater, H.S., Carey, S.K., Chun, K.P., 2016. Recent climatic, cryospheric, and hydrological changes over the interior of western Canada: a review and synthesis. Hydrol. Earth Syst. Sci. 20, 1573–1598. https://doi.org/10.5194/hess-20-1573-2016.

Dee, D.P., Uppala, S.M., Simmons, A.J., Berrisford, P., Poli, P., Kobayashi, S., Andrae, U., Balmaseda, M.A., Balsamo, G., Bauer, P., Bechtold, P., Beljaars, A.C.M., van de

Berg, L., Bidlot, J., Bormann, N., Delsol, C., Dragani, R., Fuentes, M., Geer, A.J., Haimberger, L., Healy, S.B., Hersbach, H., Hólm, E.V., Isaksen, L., Kållberg, P., Köhler, M., Matricardi, M., McNally, A.P., Monge-Sanz, B.M., Morcrette, J.-J., Park, B.-K., Peubey, C., de Rosnay, P., Tavolato, C., Thépaut, J.-N., Vitart, F., 2011. The ERA-Interim reanalysis: configuration and performance of the data assimilation system. Q. J. Roy. Meteorol. Soc. 137 (656), 553–597.

Demuth, M., Pinard, V., Pietroniro, A., Luckman, B., Hopkinson, C., Dornes, P., Comeau, L., 2008. Recent and past-century variations in the glacier resources of the Canadian Rocky Mountains: Nelson River system. Terra Glacialis Special Issue - Mountain Glaciers and Climate Changes of the Last Century, 27-52.

Ellis, C.R., Pomeroy, J.W., Brown, T., MacDonald, J., 2010. Simulation of snow accumulation and melt in needleleaf forest environments. Hydrol. Earth Syst. Sci. 14, 925–940. https://doi.org/10.5194/hess-14-925-2010.

Ellis, C.R., Pomeroy, J.W., Link, T.E., 2013. Modeling increases in snowmelt yield and desynchronization resulting from forest gap thinning treatments in a northern mountain catchment. Water Resour. Res. 49, 936–949. https://doi.org/10.1002/wrcr.20089.

Environment and Climate Change Canada, 2020. 1971-2000 Canadian Climate Normals. Available at: https://climate.weather.gc.ca/climate_normals/index_e.html, last access: 15 September 2020.

Environment and Climate Change Canada, 2023. Canadian Climate Data and Scenarios. Available at: https://climate-scenarios.canada.ca/?page=cmip5-intro, last access: 23 February 2023.

ESRI (Environmental Systems Research Institute), 1999. ArcView GIS 3.2. Environmental Systems Research Institute, Inc., Redlands, CA.

Fang, X., Pomeroy, J.W., 2016. Impact of antecedent conditions on simulations of a flood in a mountain headwater basin. Hydrol. Process. 30, 2754–2772. https://doi.org/10.1002/hyp.10910.

Fang, X., Pomeroy, J.W., 2020. Diagnosis of future changes in hydrology for a Canadian Rockies headwater basin. Hydrol. Earth Syst. Sci. 24, 2731–2754. https://doi.org/10.5194/hess-24-2731-2020.

Fang, X., Pomeroy, J.W., Westbrook, C.J., Guo, X., Minke, A.G., Brown, T., 2010. Prediction of snowmelt derived streamflow in a wetland dominated prairie basin. Hydrol. Earth Syst. Sci. 14, 991–1006. https://doi.org/10.5194/hess-14-991-2010.

Fang, X., Pomeroy, J.W., Ellis, C.R., MacDonald, M.K., DeBeer, C.M., Brown, T., 2013. Multi-variable evaluation of hydrological model predictions for a headwater basin in the Canadian Rocky Mountains. Hydrol. Earth Syst. Sci. 17, 1635–1659. https://doi.org/10.5194/hess-17-1635-2013.

Farjad, B., Gupta, A., Marceau, D.J., 2016. Annual and seasonal variations of hydrological processes under climate change scenarios in two sub-catchments of a complex watershed. Water Resour. Manage. 30, 2851–2865. https://doi.org/10.1007/s11269-016-1329-3.

Garnier, B.J., Ohmura, A., 1970. The evaluation of surface variations in solar radiation income. Sol. Energy 13 (1), 21–34.

Gizaw, M.S., Gan, T.Y., 2016. Possible impact of climate change on future extreme precipitation of the Oldman, Bow and Red Deer River Basins of Alberta. Int. J. Climatol. 36 (1), 208–224.

Gobena, A.K., Gan, T.Y., 2010. Incorporation of seasonal climate forecasts in the ensemble streamflow prediction system. J. Hydrol. 385 (1-4), 336–352.

Granger, R.J., Gray, D.M., 1990. A net radiation model for calculating daily snowmelt in open environments. Nord. Hydrol. 21, 217–234.

Granger, R.J., Pomeroy, J.W., 1997. Sustainability of the western Canadian boreal forest under changing hydrological conditions - 2-summer energy and water use. In: Rosjberg, D., Boutayeb, N., Gustard, A., Kundzewicz, Z., Rasmussen, P. (Eds.), Sustainability of Water Resources under Increasing Uncertainty. IAHS Publication No. 240. IAHS Press, Wallingford, United Kingdom, pp. 243–250.

Harder, P., Pomeroy, J., 2013. Estimating precipitation phase using a psychrometric energy balance method. Hydrol. Process. 27, 1901–1914. https://doi.org/10.1002/hyp.9799.

Harder, P., Pomeroy, J.W., Westbrook, C.J., 2015. Hydrological resilience of a Canadian Rockies headwaters basin subject to changing climate, extreme weather, and forest management. Hydrol. Process. 29, 3905–3924. https://doi.org/10.1002/hyp.10596.

Hedstrom, N.R., Pomeroy, J.W., 1998. Measurements and modelling of snow interception in the boreal forest. Hydrol. Process. 12 (10-11), 1611–1625.

Hopkinson, C., Young, G.J., 1998. The effect of glacier wastage on the flow of the Bow River at Banff, Alberta, 1951–1993. Hydrol. Process. 12 (10-11), 1745–1762.

Ipcc, 2013. In: Climate Change 2013: The Physical Science Basis, Contribution of Working Group I to the Fifth Assessment Report of the Intergovernmental Panel on Climate Change. Cambridge University Press, Cambridge, United Kingdom and New York, NY, USA, p. 1535. https://doi.org/10.1017/CBO9781107415324.

Islam, Z., Gan, T.W., 2015. Potential combined hydrologic impacts of climate change and El Niño Southern Oscillation to South Saskatchewan River Basin. J. Hydrol. 523, 34–48. https://doi.org/10.1016/j.jhydrol.2015.01.043.

Kienzle, S.W., Nemeth, M.W., Byrne, J.M., MacDonald, R.J., 2012. Simulating the hydrological impacts of climate change in the upper North Saskatchewan River basin, Alberta. Canada. J. Hydrol. 412–413, 76–89. https://doi.org/10.1016/j.jhydrol.2011.01.058.

Knowles, N., Dettinger, M.D., Cayan, D.R., 2006. Trends in snowfall versus rainfall in the Western United States. J. Clim. 19, 4545–4559.

Krinner, G., Derksen, C., Essery, R., Flanner, M., Hagemann, S., Clark, M., Zhu, D., 2018. ESM-SnowMIP: assessing snow models and quantifying snow-related climate feedbacks. Geosci. Model Dev. 11, 5027–5049. https://doi.org/10.5194/gmd11-5027-2018.

Krogh, S.A., Pomeroy, J.W., 2019. Impact of future climate and vegetation on the hydrology of an Arctic headwater basin at the tundra–taiga transition. J. Hydrometeorol. 20, 197–215. https://doi.org/10.1175/JHM-D-18-0187.1.

Krogh, S.A., Pomeroy, J.W., Marsh, P., 2017. Diagnosis of the hydrology of a small Arctic basin at the tundra-taiga transition using a physically based hydrological model. J. Hydrol. 550, 685–703. https://doi.org/10.1016/j.jhydrol.2017.05.042.

Lapp, S., Byrne, J., Townshend, I., Kienzle, S., 2005. Climate warming impacts on snowpack accumulation in an alpine watershed. Int. J. Climatol. 25 (4), 521–536.

Li, Y., Li, Z., Zhang, Z., Chen, L., Kurkute, S., Scaff, L., Pan, X., 2019. High-resolution regional climate modeling and projection over Western Canada using a Weather Research Forecasting model with a pseudo-global warming approach. Hydrol. Earth Syst. Sci. 23, 4635–4659. https://doi.org/10.5194/hess-23-4635.

López-Moreno, J.I., Pomeroy, J.W., Alonso-González, E., Morán-Tejeda, E., Revuelto, J., 2020. Decoupling of warming mountain snowpacks from hydrological regimes. Environ. Res. Lett. 15, 114006. https://doi.org/10.1088/1748-9326/abb55f.

López-Moreno, J.I., Pomeroy, J.W., Revuelto, J., Vicente-Serrano, S.M., 2013. Response of snow processes to climate change: spatial variability in a small basin in the Spanish Pyrenees. Hydrol. Process. 27, 2637–2650. https://doi.org/10.1002/hyp.9408.

Luce, C.H., Tarboton, D.G., 2010. Evaluation of alternative formulae for calculation of surface temperature in snowmelt models using frequency analysis of temperature observations. Hydrol. Earth Syst. Sci. 14, 535–543. https://doi.org/10.5194/hess-14-535-2010.

MacDonald, M.K., Pomeroy, J.W., Pietroniro, A., 2010. On the importance of sublimation to an alpine snow mass balance in the Canadian Rocky Mountains. Hydrol. Earth Syst. Sci. 14, 1401–1415. https://doi.org/10.5194/hess-14-1401-2010.

MacDonald, M.K., Pomeroy, J.W., Essery, R.L.H., 2018. Water and energy fluxes over northern prairies as affected by chinook winds and winter precipitation. Agr. Forest Meteorol. 248, 372–385. https://doi.org/10.1016/j.agrformet.2017.10.025.

Macias Fauria, M., Johnson, E.A., 2008. Climate and wildfires in the North American boreal forest. Phil. Trans. R. Soc. B 363 (1501), 2315–2327.

Mahat, V., Anderson, A., 2013. Impacts of climate and catastrophic forest changes on streamflow and water balance in a mountainous headwater stream in Southern Alberta. Hydrol. Earth Syst. Sci. 17, 4941–4956. https://doi.org/10.5194/hess-17-4941-2013.

Male, D.H., Gray, D.M., 1981. Snowcover ablation and runoff. In: Gray, D.M., Male, D.H. (Eds.), Handbook of Snow: Principles, Processes, Management and Use. Pergamon Press Canada Ltd., Toronto, Ontario, pp. 360–436.

Marks, D., Kimball, J., Tingey, D., Link, T., 1998. The sensitivity of snowmelt processes to climate conditions and forest cover during rain-on-snow: a case study of the 1996 Pacific Northwest flood. Hydrol. Process. 12 (10-11), 1569–1587.

Marsh, C.B., Pomeroy, J.W., Spiteri, R.J., 2012. Implications of mountain shading on calculating energy for snowmelt using unstructured triangular meshes. Hydrol. Process. 26, 1767–1778. https://doi.org/10.1002/hyp.9329.

Marshall, S.J., White, E.C., Demuth, M.N., Bolch, T., Wheate, R., Menounos, B., Beedle, M.J., Shea, J.M., 2011. Glacier Water Resources on the Eastern Slopes of the Canadian Rocky Mountains. Can. Water Resour. J. 36 (2), 109–134. https://doi.org/10.4296/cwrj3602823.

Marty, C., Schlögl, S., Bavay, M., Lehning, M., 2017. How much can we save? Impact of different emission scenarios on future snow cover in the Alps. The Cryosphere 11, 517–529. https://doi.org/10.5194/tc-11-517-2017.

Martz, L., Bruneau, J., Rolfe, J.T., 2007. Climate and Water: South Saskatchewan River Basin Final Technical Report. Prairie Adaptation Research Collaborative, Regina, Canada.

Monteith, J.L., 1965. Evaporation and environment. In state and movement of water in living organisms. In: 19th Symposium of the Society for Experimental Biology. Cambridge University Press, Cambridge, pp. 205–234.

Morgan, P., Heyerdahl, E.K., Gibson, C.E., 2008. Multi-season climate synchronized forest fires throughout the 20th century, northern Rockies, USA. Ecology 89 (3), 717–728.

Mori, A.S., Johnson, E.A., 2013. Assessing possible shifts in wildfire regimes under a changing climate in mountainous landscapes. Forest Ecol. Manag. 310, 875–886.

Munro, D.S., 2005. A revised Canadian perspective: progress in glacier hydrology. Hydrol. Process. 19, 231–245. https://doi.org/10.1002/hyp.5769.

Musselman, K.N., Pomeroy, J.W., 2017. Estimation of needleleaf canopy and trunk temperatures and longwave contribution to melting snow. J. Hydrometeorol. 18, 555–572. https://doi.org/10.1175/JHM-D-16-0111.1.

Musselman, K.N., Clark, M.P., Liu, C., Ikeda, K., Rasmussen, R., 2017. Slower snowmelt in a warmer world. Nat. Clim. Change 7, 214–220. https://doi.org/10.1038/NCLIMATE3225.

Nash, J.E., Sutcliffe, J.V., 1970. River flow forecasting through conceptual models. Part I – A discussion of principles. J. Hydrol. 10 (3), 282–290.

Naz, B.S., Frans, C.D., Clarke, G.K.C., Burns, P., Lettenmaier, D.P., 2014. Modeling the effect of glacier recession on streamflow response using a coupled glacio-hydrological model. Hydrol. Earth Syst. Sci. 18, 787–802. https://doi.org/10.5194/hess-18-787-2014.

Pomeroy, J., Fang, X., Ellis, C., 2012. Sensitivity of snowmelt hydrology in Marmot Creek, Alberta, to forest cover disturbance. Hydrol. Process. 26, 1892–1905. https://doi.org/10.1002/hyp.9248.

Pomeroy, J.W., Gray, D.M., Hedstrom, N.R., Janowicz, J.R., 2002. Prediction of seasonal snow accumulation in cold climate forests. Hydrol. Process. 16 (18), 3543–3558.

Pomeroy, J.W., Gray, D.M., Brown, T., Hedstrom, N.R., Quinton, W., Granger, R.J., Carey, S., 2007. The Cold Regions Hydrological Model, a platform for basing process representation and model structure on physical evidence. Hydrol. Process. 21, 2650–2667. https://doi.org/10.1002/hyp.6787.

Pomeroy, J.W., Marks, D., Link, T., Ellis, C., Hardy, J., Rowlands, A., Granger, R., 2009. The impact of coniferous forest temperature on incoming longwave radiation to melting snow. Hydrol. Process. 23, 2513–2525. https://doi.org/10.1002/hyp.7325.

Pomeroy, J.W., Fang, X., Shook, K., Whitfield, P.H., 2013. Predicting in ungauged basins using physical principles obtained using the deductive, inductive, and abductive reasoning approach. In: Pomeroy, J.W., Whitfield, P.H., Spence, C. (Eds.), Putting prediction in ungauged basins into practice. Canadian Water Resources Association, Canmore, Alberta, pp. 41–62.

Pomeroy, J.W., Fang, X., Rasouli, K., 2015. Sensitivity of snow processes to warming in the Canadian Rockies. In: Proceedings of the 72nd Eastern Snow Conference, 9–11 June 2015. Sherbrooke, Québec, Canada, pp. 22–33.

Pomeroy, J.W., Fang, X., Marks, D.G., 2016b. The cold rain-on-snow event of June 2013 in the Canadian Rockies – characteristics and diagnosis. Hydrol. Process. 30, 2899–2914. https://doi.org/10.1002/hyp.10905.

Pomeroy, J.W., Brown, T., Fang, X., Shook, K.R., Pradhananga, D., Armstrong, R., Harder, P., Marsh, C.H., Costa, D., Krogh, S.A., Aubry-Wake, C., Annand, H., Lawford, P., He, Z., Kompanizare, M., López-Moreno, J.I., 2022. The cold regions hydrological modelling platform for hydrological diagnosis and prediction based on process understanding. J. Hydrol. 615, 128711 https://doi.org/10.1016/j.jhydrol.2022.128711.

Pomeroy, J.W., Li, L., 2000. Prairie and arctic areal snow cover mass balance using a blowing snow model. J. Geophys. Res.-Atmos. 105 (D21), 26619–26634. https://doi.org/10.1029/2000JD900149.

Pomeroy, J., Stewart, R.E., Whitfield, P.H., 2016a. The 2013 flood event in the Bow and Oldman River basins: causes, assessment and damages. Can. Water Resour. J. 41 (1–2), 105–117. https://doi.org/10.1080/07011784.2015.1089190.

Pradhananga, D., Pomeroy, J.W., 2022a. Diagnosing changes in glacier hydrology from physical principles, using a hydrological model with snow redistribution, sublimation, firnification and energy balance ablation algorithms. J. Hydrol. 608, 127545 https://doi.org/10.1016/j.jhydrol.2022.127545.

Pradhananga, D., Pomeroy, J.W., 2022b. Recent hydrological response of glaciers in the Canadian Rockies to changing climate and glacier configuration. Hydrol. Earth Syst. Sci. 26, 2605–2616. https://doi.org/10.5194/hess-26-2605-2022.

Priestley, C.H.B., Taylor, R.J., 1972. On the assessment of surface heat flux and evaporation using large-scale parameters. Mon. Weather Rev. 100 (2), 81–92.

Prior, G.J., Hathway, B., Glombick, P., Pana, D.I., Banks, C.J., Hay, D.C., Schneider, C.L., Grobe, M., Elgr, R., Weiss, J.A., 2013. Bedrock geology of Alberta, AER/AGS Map 600, Alberta Energy Regulator.

Rasouli, K., Pomeroy, J.W., Whitfield, P.H., 2019a. Hydrological responses of headwater basins to monthly perturbed climate in the North American Cordillera. J. Hydrometeorol. 20, 863–882. https://doi.org/10.1175/JHM-D-18-0166.1.

Rasouli, K., Pomeroy, J.W., Whitfield, P.H., 2019b. Are the effects of vegetation and soil changes as important as climate change impacts on hydrological processes? Hydrol. Earth Syst. Sci. 23, 4933–4954. https://doi.org/10.5194/hess-23-4933-2019.

Rasouli, K., Pomeroy, J.W., Whitfield, P.H., 2022. The sensitivity of snow hydrology to changes in air temperature and precipitation in three North American headwater basins. J. Hydrol. 606, 127460 https://doi.org/10.1016/j.jhydrol.2022.127460.

Rood, S.B., Pan, J., Gill, K.M., Franks, C.G., Samuelson, G.M., Shepherd, A., 2008. Declining summer flows of Rocky Mountain rivers: Changing seasonal hydrology and probable impacts on floodplain forests. J. Hydrol. 349, 397–410. https://doi.org/10.1016/j.jhydrol.2007.11.012.

Scaff, L., Prein, A.F., Li, Y., Clark, A.J., Krogh, S.A., Taylor, N., Liu, C., Rasmussen, R.M., Ikeda, K., Li, Z., 2021. Dryline characteristics in North America's historical and future climates. Clim. Dyn. 57 (7-8), 2171–2188.

Schirmer, M., Jamieson, B., 2015. Verification of analysed and forecasted winter precipitation in complex terrain. The Cryosphere 9, 587–601. https://doi.org/10.5194/tc-9-587-2015.

Schirmer, M., Pomeroy, J.W., 2020. Processes governing snow ablation in alpine terrain – detailed measurements from the Canadian Rockies. Hydrol. Earth Syst. Sci. 24, 143–157. https://doi.org/10.5194/hess-24-143-2020.

Schmidt, R.A., Gluns, D.R., 1991. Snowfall interception on branches of three conifer species. Can. J. Forest Res. 21 (8), 1262–1269.

Shea, J.M., Marshall, S.J., Livingston, J.M., 2004. Glacier distributions and climate in the Canadian Rockies. Arct. Antarct, Alp. Res. 36 (2), 272–279.

Shea, J.M., Whitfield, P.H., Fang, X., Pomeroy, J.W., 2021. The role of basin geometry in mountain snowpack responses to climate change. Front. Water 3, 604275. https://doi.org/10.3389/frwa.2021.604275.

Shook, K., 2016. The 2005 flood events in the Saskatchewan River Basin: causes, assessment and damages. Can. Water Resour. J. 41 (1–2), 94–104. https://doi.org/10.1080/07011784.2014.1001439.

Shook, K., Pomeroy, J., 2012. Changes in the hydrological character of rainfall on the Canadian Prairies. Hydrol. Process. 26, 1752–1766. https://doi.org/10.1002/hyp.9383.

Sicart, J.E., Pomeroy, J.W., Essery, R.L.H., Bewley, D., 2006. Incoming longwave radiation to melting snow: Observations, sensitivity and estimation in northern environments. Hydrol. Process. 20, 3697–3708. https://doi.org/10.1002/hyp.6383.

Sillmann, J., Kharin, V.V., Zwiers, F.W., Zhang, X., Bronaugh, D., 2013. Climate extremes indices in the CMIP5 multimodel ensemble: Part 2. Future climate projections. J. Geophys. Res. Atmos. 118, 2473–2493. https://doi:10.1002/jgrd.50188.

Smith, C.D., 2008. The Relationship between monthly precipitation and elevation in the Alberta foothills during the foothills orographic precipitation experiment, in: Woo, M. (Ed), Cold Region Atmospheric and Hydrologic Studies, The Mackenzie GEWEX Experience, Volume 1: Atmospheric Dynamics. Springer, Berlin, Heidelberg, pp. 167-185.

Soil Landscapes of Canada Working Group. 2011. Soil Landscapes of Canada version 3.2. Agriculture and Agri-Food Canada.

Tanzeeba, S., Gan, T.Y., 2012. Potential impact of climate change on the water availability of South Saskatchewan River Basin. Climatic Change 112 (2), 355–386.

Taylor, K.E., Stouffer, R.J., Meehl, G.A., 2012. An overview of CMIP5 and the experiment design. B. Am. Meteorol. Soc. 93, 485–498. https://doi.org/10.1175/BAMS-D-11-00094.1.

Tennant, C., Menounos, B., Wheate, R., Clague, J.J., 2012. Area change of glaciers in the Canadian Rocky Mountains, 1919 to 2006. The Cryosphere 6, 1541–1552. https://doi.org/10.5194/tc-6-1541-2012.

Thériault, J.M., Hung, I., Vaquer, P., Stewart, R.E., Pomeroy, J.W., Precipitation characteristics and associated weather conditions on the eastern slopes of the Canadian Rockies during March–April 2015. Hydrol. Earth Syst. Sci. 22, 4491–4512. https://doi.org/10.5194/hess-22-4491-2018.

Valeo, C., Xiang, Z., Bouchart, F.J., Yeung, P., Ryan, M.C., 2007. Climate change impacts in the Elbow River watershed. Can. Water Resour. J. 32, 285–302. https://doi.org/10.4296/cwrj3204285.

van Vuuren, D.P., Edmonds, J., Kainuma, M., Riahi, K., Thomson, A., Hibbard, K., Hurtt, G.C., Kram, T., Krey, V., Lamarque, J.-F., Masui, T., Meinshausen, M., Nakicenovic, N., Smith, S.J., Rose, S.K., 2011. The representative concentration pathways: an overview. Climatic Change 109 (1-2), 5–31.

Verseghy, D., 2012. CLASS - The Canadian land surface scheme (version 3.6), Technical Documentation. Climate Research Division, Science and Technology Branch, Environment Canada, pp 179.

Vionnet, V., Belair, S., Girard, C., Plante, A., 2015. Wintertime subkilometer numerical forecasts of near-surface variables in the Canadian Rocky Mountains. Mon. Weather Rev. 143, 666–686. https://doi.org/10.1175/MWR-D-14-00128.1.

Vionnet, V., Fortin, V., Gaborit, E., Roy, G., Abrahamowicz, M., Gasset, N., Pomeroy, J. W., 2020. Assessing the factors governing the ability to predict late-spring flooding in cold-region mountain basins. Hydrol. Earth Syst. Sci. 24, 2141–2165. https://doi.org/10.5194/hess-24-2141-2020.

Viviroli, D., Dürr, H.H., Messerli, B., Meybeck, M., Weingartner, R., 2007. Mountains of the world, water towers for humanity: typology, mapping, and global significance. Water Resour. Res. 43 (7), W07447. https://doi.org/10.1029/2006WR005653.

Walter, M.T., Brooks, E.S., McCool, D.K., King, L.G., Molnau, M., Boll, J., 2005. Process-based snowmelt modeling: does it require more input data than temperature-index modeling? J. Hydrol. 300 (1-4), 65–75.

Wang, S., Yang, Y., Luo, Y., Rivera, A., 2013. Spatial and seasonal variations in evapotranspiration over Canada's landmass. Hydrol. Earth Syst. Sci. 17, 3561–3575. https://doi.org/10.5194/hess-17-3561-2013.

Wayand, N.E., Marsh, C.B., Shea, J.M., Pomeroy, J.W., 2018. Globally scalable alpine snow metrics. Rem. Sens. Environ. 213, 61–72.

Westerling, A.L., Hidalgo, H.G., Cayan, D.R., Swetnam, T.W., 2006. Warming and earlier spring increase western U.S. forest wildfire activity. Science 313 (5789), 940–943.

Whitfield, P.H., Pomeroy, J.W., 2016. Changes to flood peaks of a mountain river: implications for analysis of the 2013 flood in the Upper Bow River. Canada. Hydrol. Process. 30, 4657–4673. https://doi.org/10.1002/hyp.10957.

Whitfield, P.H., Pomeroy, J.W., 2017. Assessing the quality of the streamflow record for a long-term reference hydrometric station: Bow River at Banff. Can. Water Resour. J. 42 (4), 391–415. https://doi.org/10.1080/07011784.2017.1399086.

Williams, T.J., Pomeroy, J.W., Janowicz, J.R., Carey, S.K., Rasouli, K., Quinton, W.L., 2015. A radiative–conductive–convective approach to calculate thaw season ground surface temperatures for modelling frost table dynamics. Hydrol. Process. 29, 3954–3965. https://doi.org/10.1002/hyp.10573.

Wood, W.H., Marshall, S.J., Whitehead, T.L., Fargey, S.E., 2018. Daily temperature records from a mesonet in the foothills of the Canadian Rocky Mountains, 2005–2010. Earth Syst. Sci. Data 10, 595–607. https://doi.org/10.5194/essd-10-595-2018.

Woods, A., Coates, K.D., Hamann, A., 2005. Is an unprecedented dothistroma needle blight epidemic related to climate change? BioScience 55, 761–769.

Xie, C., Gough, W.A., 2013. A simple thaw-freeze algorithm for multi-layered soil using the Stefan equation. Permafrost Periglac. 24, 252–260. https://doi.org/10.1002/ppp.1770.

Zhang, X., Vincent, L.A., Hogg, W.D., Niitsoo, A., 2000. Temperature and precipitation trends in Canada during the 20th century. Atmosphere-Ocean 38 (3), 395–429.

Zhao, L., Gray, D.M., 1999. Estimating snowmelt infiltration into frozen soils. Hydrol. Process. 13 (12-13), 1827–1842.